12-2012

Application of Response Surface Methodology and Central Composite Design for 5P12-RANTES Expression in the *Pichia pastoris* System

Frank M. Fabian
University of Nebraska-Lincoln, frankfabsan@gmail.com

APPLICATION OF RESPONSE SURFACE METHODOLOGY AND CENTRAL COMPOSITE DESIGN FOR 5P12-RANTES EXPRESSION IN THE *Pichia pastoris* SYSTEM

By

Frank M. Fabian

A THESIS

Presented to the Faculty of

The Graduate College at the University of Nebraska

In Partial Fulfillment of Requirements

For the Degree of Master of Science

Major: Chemical Engineering

Under the Supervision of Professor William H. Velander

Lincoln, Nebraska

December, 2012

APPLICATION OF RESPONSE SURFACE METHODOLOGY AND CENTRAL COMPOSITE DESIGN FOR 5P12-RANTES EXPRESSION IN THE *Pichia pastoris* SYSTEM

Frank M. Fabian, M.S.

University of Nebraska, 2012

Adviser: William H. Velander

Pichia pastoris has demonstrated the ability to express high levels of recombinant heterologous proteins. Protein expression is enhanced during fermentation at high cell density. However, the level of expression is mainly regulated by fermentation operation factors. This research is directed to investigate the effect of methanol growth rate, temperature and pH in the expression of the total 5P12-Rantes concentration, expression of active 5P12-Rantes and Specific yield using the response surface methodology and central composite design.

The response surface methodology, RSM, has been used successfully used by Zhang, W. and Ian, M. to optimize the cell density and fermentation process. The RSM is equipped with statistical tools to determine the significance of a factor over a response. The evaluation of factors using the RSM uses experimental design in order to distribute the selected variables within the boundaries of the design.

The central composite design, CCD, allows allocation of Methanol growth rate, temperature, and pH to evaluate their effect in the expression of 5P12-Rantes. The effect of methanol growth rate is evaluated from a minimum value of 0.01 h^{-1} to a maximum of 0.4 h^{-1}, 24.06 °C to 29.94 °C for temperature and 1.99 to 4.51 for pH.

The methanol growth rate has demonstrated to have no effect in any of the responses. In contrast, Temperature and pH has a significant effect in all the responses. However, the lack of fit of the proposed model doesn't allow good estimations of predicted responses. In order to minimize the lack of fit of the propose models, the methanol growth rate has been excluded from all the three models. A new 2 factor second order model is proposed to analyze the significance of temperature and pH. The lack of fit decreased and the optimal operating conditions for temperature and pH was determined at 27.14 ℃ and 3.16 which results in a maximum of 26.52 g/L of active 5P12-Rantes and 0.16 mg Rantes/g dry cell.

Acknowledgements

This work was founded by the MINTAKA medical research foundation and the College on Engineering – University of Nebraska – Lincoln through the Chemical Engineering Department. I want to express my sincere gratitude to Dr. William Velander for his support and guidance towards the completion of this project. It's pretty satisfactory to meet persons like Dr. Velander whose inspiration for science help others to get their objectives and goals in life. This project wouldn't be possible without the initial opportunity that Dr. Michael Meagher gave me two years ago. After working for him for about four years, he encourages me to know the science behind fermentation. I'm very grateful for his initial support and his reliance in my person.

I also feel indebted to all lab personal at the Biological Process Development Facility for their support. It has been really a pleasure to work with Jay Harner, Scott Johnson, Bob Sealock, Anthony Sump, John Harms and Dustin Peterson. I also want to thank Cory Smathers for his cooperation on the financial subjects and Dr. Anna Oommen (Meena) for her scientific insights.

I want to thank Dr. Mehmet Inan at the Akdeniz University at Turkey for his cooperation during codon optimization, sequence design and his generous scientific contribution in fermentation development.

I would like to thank to Dr. Kent M Eskridge at the UNL-Statistical department for his cooperation in the experimental design. Special thanks to Dr. Levon Abrahamyan at the UNL-Virology Center for his generous contribution in explaining the HIV entry

mechanism. Dr. Paul Blum and his lab team at the UNL-Biological Science Department for their support in the clonal linage development.

My deepest thanks go to my wife Rosie for her unconditional love and support throughout this journey, to my daughter Brianna and my son Ian for their love and patience. My appreciation goes to my mother Vilma and my sisters Sarella and Brenda for their emotional support.

Ultimately, it is God who drives my life and gave me the opportunity to work with all these wonderful persons.

TABLE OF CONTENTS

LIST OF FIGURES

LIST OF TABLES

CHAPTER I

LITERATURE REVIEW

ABSTRACT

The characterization of the HIV-1's envelope proteins has provided an abundant knowledge about the viral structure conformation. However, the discovery of the infection mechanism has made possible the development of drugs to prevent HIV-1 infection. The sequence of HIV-1 infection is mainly characterized by a series of conformational modifications in the viral envelope proteins. These modifications direct the interaction of the virus with the target cell and thereafter the delivery the RNA viral information.

Human cells express an incredible variety of proteins directed to protect them against diseases. For example, Regulated-on-Activation-Normal-T-cells-Expressed-and-Secreted, RANTES, has chemoattractant activity for monocytes and it is expressed in response to viral infection. This protein is expressed by the immune cells called cytotoxic phenotype CD8+ and the helper CD4+ T cell in response to the detection of a foreign microorganism. Unfortunately, in the case of HIV-1, the expression of RANTES occurs after the cells have been infected by the virus.

The development of effective therapies to protect against HIV-1 viral infection has focused upon the design of drugs with the capability to interfere with the infection mechanism. For example, 5P12-Rantes, a homologous of human RANTES, has proved protection against HIV-1 infection by competitive interaction with the co-receptor CCR5.

The chapter discusses the HIV-1 entry mechanism and describes the conformational modifications of the viral envelope proteins. The functional activity of the 5P12-Rantes is described as part of viral entry inhibition.

INTRODUCTION

HIV-1 Entry Mechanism

The HIV-1entry mechanism depends on the sequential interaction of the virion envelope glycoproteins 120 and 41 (gp120 and gp41) with cellular receptor cluster of differentiation (CD4) and co-receptor chemokine type 5 or CCR5 (Rizzuto et al. 1998). Initially, the virion binds to the host cell receptor (T cells) by non-covelant interaction between the virion surface envelope glycoprotein, gp120, and the protein receptor, CD4. Once CD4 binds the virion envelope glycoprotein gp120, the later undergoes a change in its conformation that enables it to engage the co-receptor CCR5. This step then triggers fusion of the virus with the cell membrane (Wilen et al. 2012). Finally, gp120 dissociates from the membrane-anchored gp41. Then, gp41 refolds in a series of sequential steps that leads to a closer contact of the viral envelop (Env) with the cell membrane (Liu, et al. 2008). The viral core is then delivered into the host cell. (Chen, et al. 2005)

The primary and tertiary structure and of both the virion envelope glycoprotein, gp120, and the cell receptor, CD4, play an important role in the ultimate formation of the envelope complex. (Wu,et al 1996) The virion envelope glycoprotein structure is showed in Figure 1.1. The gp120 , synthesized in the endoplasmic reticulum, consists of 25 β-strands, 5α helices and 10 defined loop segments (Kwong et al. 1998). The gp120 is found as trimers on the surface of the viral membrane.(Liu, et al 2008) and it is folded

into two major domains: five highly conserved inner domains (C1-C5) and five hyper variable loops (V1-V5). The conserved domains are important for gp120 folding and binding of the co-receptor, CCR5 (Rizzuto et al. 1998), the variable domains are involved in immune evasion and conformational modifications. (Wilenet al.2012)

The cellular receptor CD4 is an immunoglobin protein conformed of three regions: an extracellular region, a hydrophobic trans membrane domain, and a highly charged cytoplasmic domain containing 370, 26, and 38 amino acid residues respectively. (Capon et al. 1991) The extracellular region of CD4 contains four recognized immunoglobin (Ig)-like domains denoted D1,D2,D3 and D4. (Harrison et al. 1992). D1 and D2, showed in Figure 1.2, are defined as the membrane distal two-domain fragment; meanwhile D3 and D4 are known as the membrane proximal two-domain fragment. In particular the D1 domain contains a specific binding site for the glycoprotein, gp120 (Wu et al. 1996)

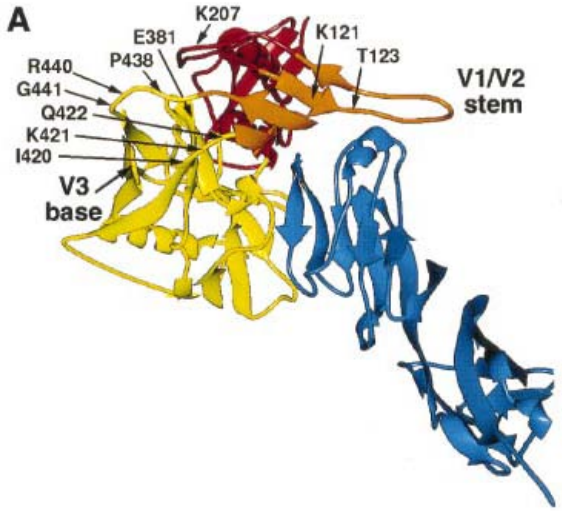

Figure 1.1: A ribbon drawing of the HIV-1 glyco protein 120 (gp120)

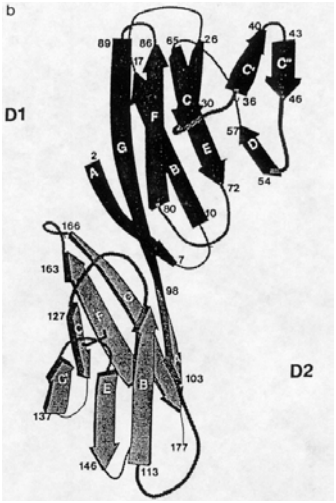

Figure 1.2: Ribbon diagram showing organization of the distal two domain fragment D1and D2 of the CD4 cellular receptor

GP120 undergoes a change in its structural conformational after binding the protein receptor CD4. This complex is mediated by chemokine receptor CCR5. (Kwong, et al., 1998). The D1-D2 extracellular fragment of CD4 the receptor protein binds gp120 in a depressed region formed at the interface of the outer domain with the inner domain and the bridging sheet of the gp120 (Figure 1.3). This region is surrounded by carbohydrate moieties and is partially occluded by the flexible loops V1 and V2. (Wilen. et al. 2012). The molecular interaction between CD4 and gp120 occurs by direct interatomic contacts between 22 CD4 amino acids residues and 26 gp120 amino acid residues which results in 219 van der Waals contacts and 12 hydrogen bonds. The most important interactions, Phe43 and Arg59 of CD4 make multiple contacts on residues Asp368, Glu370, and Trp427 of gp120. (Kwong, et al., 1998) These interactions induce the conformational modification of the conserved inner domain of gp120 promoting the independent moving of each domain (Chen, et al. 2005) This modification is enhanced

by the flexibility of the D1-D2 domains of CD4 (Liu, et al 2008) The overall modification induced by these interactions causes:a 30° rotation of the three strand antiparallel sheet , the formation of four-stranded bridging sheet , and the displacement of the four-turn α-helix away from the outer domain (Figure 1.4). (Chen, et al. 2005). As a result, the V3 loop region is released from the lateral edge of the glycoprotein 120 and oriented into the target cell (Liu, et al 2008).

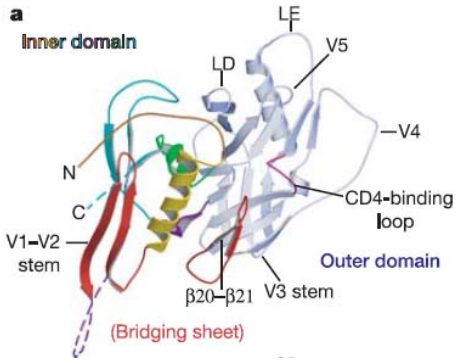

Figure 1.3: Un-ligated SIV gp120 core structure

The complex formed during the interaction of gp120 and CD4 causes viral proteins to bind the chemokine co-receptor type 5 (CCR5) (Wilen et al. 2012). CCR5 is a trans membrane protein that contains 352 amino acids and has a molecular mass of 40.6 kDa (Figure 1.5). The CCR5 has 3 external closed loops (ECL1, ECL2, ECL3) and 4 internal closed loops (ICL1, ICL2, ICL3, ICL4). This chemokine receptor is expressed in T-lymphocytes with memory/effector phenotype, monocytes, macrophage, and immature dentritic cells. The amino acids aspartic acid and glutamic acid at the N-terminal of CCR5 confer acidic properties to CCR5 (Oppermann et al. 2004). Additional negative charges are conferred by sulfation of tyrosine residues at positions 3,10,14 and 15(Farzan et al. 1999) and improves the capability of CCR5 to interact with the envelope

glycoprotein, gp120. (Oppermann et al. 2004). Furthermore, tyrosine-sulfated residues in the N-terminal of CCR5 bind the V3 loop and the bridging sheet. In order to bind the sulfated tyrosine residue at the CCR5 receptor, the V3 loop is modified into a rigid β-hairpin by additional conformational changes of the gp120 (Huang et al. 2007) caused by formation of numerous hydrogen bonds in the V3 loop. (Wilen et al. 2012)

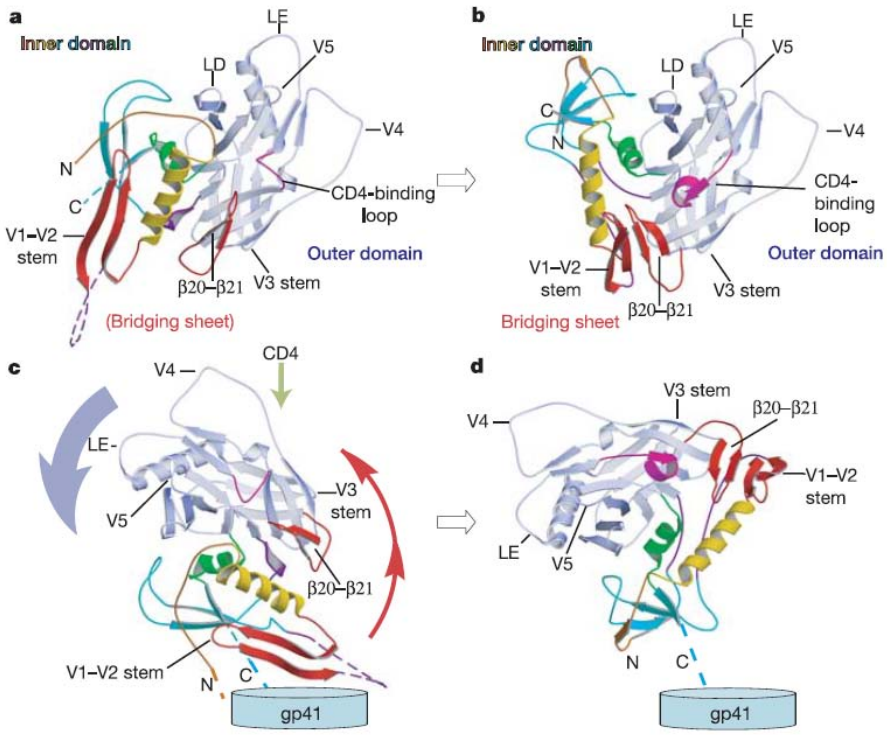

Figure 1.4: Conformational changes in the gp120 during binding of the protein receptor CD4.

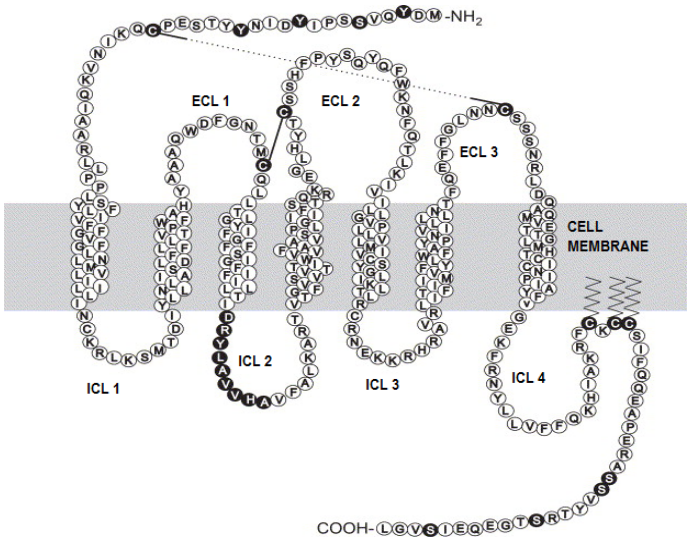

Figure 1.5: Two dimensional topology of the Human CCR5 sequence.

The viral genomic load is delivered to the cell by a generalized “cast-and-fold” fusion mechanism induced by a conformational change of the glycoprotein, gp41. (Melikyan et al, 2008). The core of gp41 , showed in Figure 1.6, is composed of a trimer of two interacting peptides. Structurally, the gp41 is formed by six helical bundles. The internal N-terminal helical regions (HR-N) is formed of three parallel coiled-coiled trimer, meanwhile the C-terminal helical regions (HR-C) are packed in an oblique, antiparallel manner to form highly conserved, hydrophobic grooves in the surface of this trimer. (Chan et al, 1997).The result is a highly stable six-helix bundle (6HB) (Wilen et al, 2012). However, a delivery pore is initially catalyzed by pre-bundle and energetically unstable structures. These occurs in the HR1 and HR2 regions and are critical for fusion. (Melijyan et al. 2008) The early pre-bundle is characterized by the maximization of the distance between HR-N and HR-C. Meanwhile, the late pre-bundle describe the formation of the nascent fusion pore (Wilen et al. 2012). Finally, the 6HB dilates the

delivery pore to a size that permits the transfer of the viral load (Figure 1.6). (Melikyan, et al 2008)

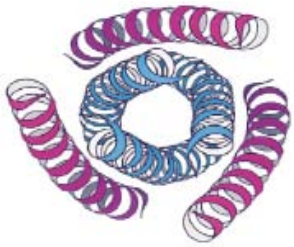

Figure 1.6: HR-C and HR-N of the gp41

Inhibition of HIV entry

Inhibition of the HIV entry mechanism can occur at any of the three major steps of the interaction between the viral envelope proteins and cell membrane protein receptors. The inhibition of the attachment and binding of receptor CD4, binding of co-receptor CCR5, and membrane fusion are the principal focus for the development of drugs that can limit the infectivity of the virus. (Wilen et al. 2012).The discovery of mechanistically novel HIV-1 inhibitors has resulted in the development of new drugs like *Enfuvirtide* (Meanwell et al. 2003) and *Maraviroc* (Lieberman-Blum et al. 2008) that interfere with the function of gp41 and CCR5 interaction respectively. Although these drugs are relative important to prevent the HIV entry, the study of the inhibition of the three other stages of entry mechanism is also to understand the drug activity and design (Wiley et al. 2012).

Several anionic polymers have been shown to inhibit the attachment and binding of gp120 with CD4. These anionic organic compounds that include various naphthalene disulfonates disrupt the interaction of the gp120–CD4 that suppresses the efficiency of

HIV-1 infection (Rusconi et al. 1996). These polymers are directed to prevent the electrostatic interaction between the positively charged viral envelope and the negatively charged cell surface. However, these polymers have not in vivo efficacy when used as vaginal microbicide (Wiley et al. 2012). In contrast, other drugs which target the CD4 binding site in gp120 have shown promising activity to prevent further interaction between the viral envelope and the CD4 receptor. For example, BMS-378806 is a small molecule that binds gp120 and inhibits the interaction of the envelope protein and the cellular receptor (Lin et al. 2003). Another small molecule drug, BMS-488043 directly inhibits the conformational changes of the CD4 and CCR5 binding sites in the gp120. (Ho et al. 2006).

The discovery of resistance to HIV-1 infection in individuals with mutation in CCR5 demonstrates that this co-receptor is essential element of virus – cell membrane fusion. The mutant allele the CCR-5, *Δccr-5*, prevents membrane fusion (Libert et al, 1998). A 32-bp deletion within the coding sequence in the region that corresponds to the second extracellular loop has been identified as the mutation region (Samson et al. 1996). Hence, the development of new drugs is directed towards the inhibition of the co-receptor CCR5. For example, *Maraviroc*, has been approved for human use in 2007 by the FDA as well as other CCR5 antagonists that bind a hydrophobic pocket in the trans-membrane domain of the CCR5. These antagonists bind not at the region in which V3-gp120 interacts with the co-receptor, but likely in a way that induces allosteric modification of the second extracellular loop and consequently prevents the cellular fusion (Baba et al. 1999). Interestingly, the chemokine receptor CCR-5 interacts with some natural native secreted proteins such as macrophage-inflammatory-protein (MIP)-1α, MIP-1β and

RANTES to block the HIV-1 infection. However, nonpeptide CCR5 antagonists have been also discovered. Thus, there is a need to develop other CCR5 antagonists for inhibition of the CCR5 interaction (Wilen et al. 2012).

Cell fusion inhibitors are directed to bind the viral envelope glycoprotein gp41 and prevent the formation of the fusion pore. For example, *Enfuvirtide,* a 36 amino acid peptide, binds directly to the HR-N region and prevents the formation of the hair pin structure that enhances the formation of the fusion pore. (Moyle et al. 2003). However, this drug has demonstrated to be ineffective against some strains that present mutation in the HR-N region of the virus (Wiley et al. 2012). Another set of drugs that inhibit the functionality of the glycoprotein, gp41, are D-peptides. These D-peptides target the hydrophobic pocket of the gp41 as *Enfuvirtide* prevents the formation of the hair pin structure of gp41 (Welch et al.2007).

RANTES Expression, regulation, and HIV entry inhibition

Regulated-on-Activation-Normal-T-cells-Expressed-and-Secreted (RANTES) is a pro inflammatory human native protein that belongs to the chemokine family proteins and has high affinity to CCR5 receptors in T cells. RANTES is expressed in cytotoxic CD8+ phenotype and the helper CD4+ T cells as a response to inflammatory viral infection (Song et al. 2000). Once cells have been activated by antigen binding, RANTES mRNA is induced after three to five days of activation. This late expression is characterized by a change in the expression patterns of T cells needed for T lymphocytes cells to a mature. The human RANTES gene has been located on chromosome 17 and composed of three exons and two introns (Figure 1.7) (Nelson, et al 1993). In addition,

the RANTES Factor of Late Activated T Lymphocytes-1 (RFLAT-1) works as an activator in the RANTES promoter cis-acting binding and regulates its expression. The RFLAT-1 belongs to the family of zinc finger transcription factors (Song et al. 1999).

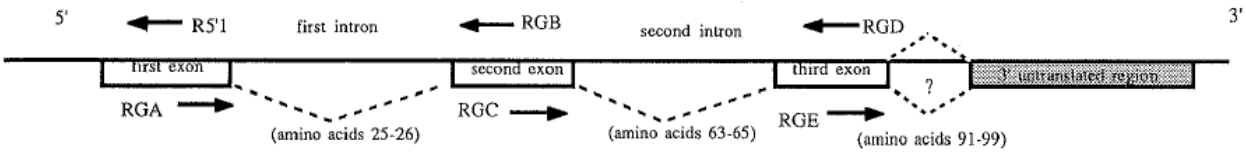

Figure 1.7: Human RANTES introns and exons

RANTES is a member of the CC chemokine family that forms a stable dimer at neutral pH and has the tendency to aggregate at pH 4.0. Each monomer contains a C-terminal α-helix packed against a three-stranded antiparallel β-sheet and two short N-terminals β-strand (Figure 1.8). The N-terminal regions are considered important to dimer formation (Skelton et al. 1995). RANTES has four cysteine residues contained in a 68 amino acids polypeptide. Two adjacent cysteine residues form the characteristic CC sequence of chemokine family members (Figure 1.9) (Nishiyama et al. 2002).

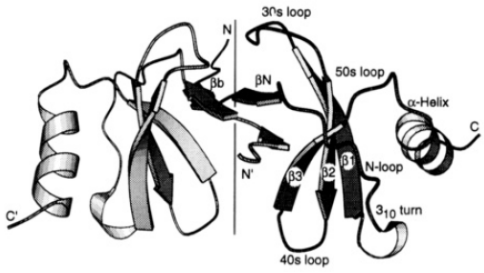

Figure 1.8: dimer structure of RANTES

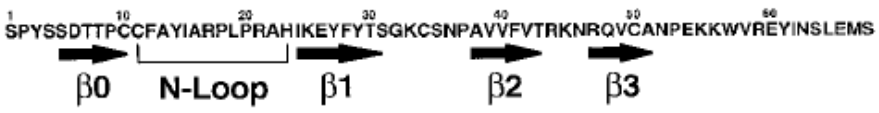

Figure 1.9: Amino acid sequence of human RANTES

RANTES function in the recruitment of T cells to the inflamed tissue and is a powerful chemoattractant for many other cells as monocytes, NK cells, memory T cells, eosinophils, and dendritic cells (Crawford et al, 2011). The high affinity between CCR5 receptor and RANTES make inhibition of the infection by HIV-1. RANTES, MIP-1α and MIP-1β, are considered a suppressive factors during HIV-1 infection (Cocchi et al 1995). It is known that aggregation of RANTES is important for chemotaxis activity even though the physiological dimeric structure of RANTES has not been well defined (Appay et al. 2000). RANTES possesses two distinct regions that have been identified as the regions that interact with the chemokine receptor, CCR5. The N-terminal and the N-loop region are the regions that have demonstrated interaction with the HIV's co-receptor, CCR5 (Nardese et al. 2001). The N-loop residues Phe 12, Ile 15, and Tyr 27 – Tyr 29, (Figure 1.10) have been identified as contributors to the formation of large hydrophobic, solvent exposed patches that provide a high docking interaction with the trans-membrane protein, CCR5 (Nardese et al, 2001).

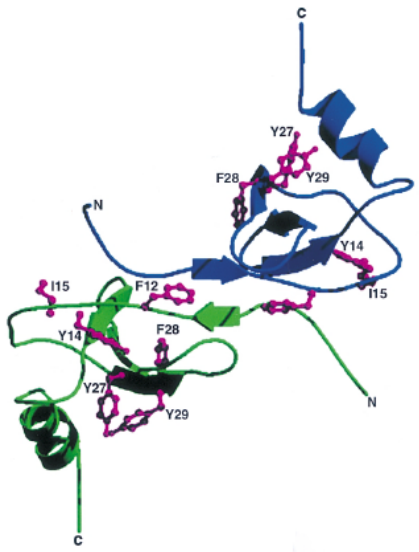

Figure 1.10: Dimeric structure of RANTES and critical amino acids residues

RANTES chemokine analogues

New HIV-1 preventive and protective drugs used as microbicides are being developed on mucosal surfaces to decrease the sexual transmission of the HIV. In that context, RANTES is a natural inhibitor to prevent and block the entry mechanism of the tropic HIV-1. Even though there is not universal agreement about the entry mechanism in mucosal surface, the HIV-1 co-receptor CCR5 is known to be involved in the entry process. Thus, the focus of research and development has been directed to the discovery of effective microbicides that possess analogous function as the native RANTES (Lederman et al, 2004).

Aminooxypentane (AOP)-RANTES is one of the first analogue antagonists of CCR5 developed to protect macrophage and lymphocytes from infection. AOP-RANTES was generated by the addition of an aldehyde-like group at the amino terminus of native RANTES and then reacting with aminooxypentane. This peptide offers strong inhibition of the co-receptor CCR5 and does not induce chemotaxis (Simmons et al, 1997).

Another RANTES analog, N^{α}-(n-nonanoyl)-des-Ser^{1}-[L-$thioproline^{2}$,L-α-$cyclohexyl\text{-}glycine^{3}$]RANTES (PSC-RANTES) introduce a nonanoyl group, thioproline and cyclohexylglycine in the position that correspond to the first three amino acids (Ser,Pro,Tyr) of the native RANTES. Initially tested in rhesus macaques, PSC-RANTES has resulted in the depletion of free CCR5 co-receptors (Lederman et al, 2004) This discovery has led to the likelihood that PSC-RANTES involves long-term intracellular sequestration of CCR5 and also a strong CCR5 signaling activity (Hubert et al, 2008).

Further investigation of the PSC-RANTES has demonstrated to be fifty times more potent than AOP-RANTES (Hartley et al, 2004).

PSC-RANTES is a potentially microbicide that raise the potential for a more affordable and environmentally stable compounds. Although, PSC-RANTES has demonstrated both high signaling activity and co-receptor sequestration, it has the tendency to produce inflammation which enhances the chance for HIV-infection. Two analogs called 5P12-RANTES and 6P4-RANTES have been identified using PSC-RANTES as the platform molecule (Hubert et al, 2008). 5P12-RANTES features high anti-HIV activity but no CCR5 signaling and no CCR5 sequestration. However, 6P4-RANTES offers high anti-HIV activity, high CCR5 signaling activity and high CCR5 sequestration. Both analogues offer high resistance to hydrolysis at temperature in the range of 40 to 55°C. In addition, both are very stable at acidic vaginal pH (4.0) and have resistance to degradation during incubation with human cervicovaginal lavage and human semen (Cerini et al, 2008). However, the principal characteristic of both analogues is the primary structure that contains naturally occurring amino acids. This makes them suitable for large scale recombinant production by using microorganism such as yeast (Hubert et al, 2008).

References

Appay, V., Dunbar, P., Cerundolo, V., McMichael, A., Czaplewski, L., Rowland, J. (2000) RANTES activates antigen-sprecific cytotoxic T lymphocytes in a mitogen-like manner through cell surface aggregation (2000) International Immunology, 12,1173-1182.

Baba, M., Nishimura, O., Naoyuki, K., Okamoto, M., Sawada, H., Iizawa, Y., Shiraishi, M., Aramaki, Y., Okonogi, K., Ogawa, Y., Meguro, K.,Fujino, M. (1999) A small molecule, nonpeptide CCR5 antagonist with highly potent and selective anti-HIV-1 activity. ProcNatlAcadSci USA,96,5698-5703.

Capon, D., Ward, R., (1991) The CD4-gp120 Interactions and AIDS pathogenesis.Annu. Rev. Immunol. 9,649-678.

Cerini, F., Landay, A., Gichinga, C., Lederman, M., Flyckt, R., Starks, D., Offord, R., Le Gal, F., Hartley, O., (2008) Chemokine Analogues show suitable stability for development as microbicides, Journal of Acquired Immune deficiency Syndromes. 49, 472-476

Chan, D., Fass, D., Berger, J., Kim, P., (1997) Core Structure of gp41 from the HIV Envelope Glycoprotein, Cell,89,263-273

Chen, B., Vogan, E., Gong, H., Skehel, J., Wiley, D., Harrison, S. (2005) Structure of an unliganded simian immunodeficiency virus gp120 core. Nature.433, 834-841

Cocchi, F., DeVico, A., Garzino-Demo, A., Arya, S., Gallo, R., Lusso, P. (1995) Identification of RANTES, MIP-1α and MIP-1β as the major HIV- Suppressive factors produced by CD8+ T Cells (1995), Science,270,1811-1915.

Crawford, A., Angelosanto, J., Nadwodny, K., Blackburn, S., Wherry, E. (2011) A role for the Chemokine RANTES in Regulating CD8 T Cell Response during Chronic Viral Infection, PLoS Pathogens, 7

Farzan, M., Mirzabekov, T., Kolchinsky, P., Wyatt, R., Cayabyab, M., Gerard, N., Gerard, C., Sodroski, J., Choe, H., (1999) Tyrosine Sulfation of the Amino Terminus of CCR Facilitates HIV-Entry

Harrison, S., Wang,J., Yan, Y., Garret, T., Liu, J., Moebius, U., Reinherz, E., (1992) Structure and Interactions of CD4. Cold Spring Harbor Symposia on Quantitative Biology.57,541-548.

Hartley, O., Gaertner, H., Wilken, J., Thompson, D., Fish, R., Ramos, A., Pastore, C., Dufour, B., Cerini, F., Melotti, A., Heveker, N., Picard, L., Alizon, M., Moiser, D., Kent, S., Offord, R. (2004) Medicinal chemistry applied to a synthetic protein: Development of highly potent HIV entry inhibitors, PNAS, 101, 16460 -16465.

Ho, HT., Fan, L., Nowicka-Sans B., McAuliffe, B.,Li, C-B.,Yamanaka, G., Zhou, N.,Fang, H.,Dicker, I.,Dalterio, R.,Gong, F.,Wang, T., Yin, Z.,Ueda, Y., Matiskella, J., Kadow, J., Clapham, P., Robinson, J.,Colonno, R., Lin PF. (2006) Envelope conformational changes induced by human immunodeficiency virus type I attachment inhibitors prevent CD4 binding and downstream entry events. J. Virology,80,4017-4025.

Huang, C., Lam, S., Acharya, P., Tang, M., Xiang, S., Hussan, S., Satnfield, R., Robinson, J., Sodroski, J., Wilson, I., Wyatt, R., Bewley, C., Kwong, P., (2007) Structures of the CCR5 N terminus and of a Tyrosine-sulfated antibody with HIV-1 gp120 and CD4, Science,317,1930-1934.

Hubert, G., Cerini, F., Escola, J, Kuenzu, G., Melotti, A., Offord, R., Rossito-Borlat, I., Nedellec, R., Salkowitz, J., Gorochov, G., Mosier, D., Hartley, O. (2008) Highly potent, fully recombinant anti-HIV chemokines: Reengineering a low-cost microbicide. PNAS, 105, 17706-17711.

Lederman, M., Veazey, R., Offord, R., Moiser, D., Dufour, J., Mefford, M., Piatak, M., Lifson, J., Salkowitz, J., Rodriguez, B., Blauvelt, A., Hartley, O. (2004) Prevention of vaginal SHIV transmission in Rhesus Macaques trough inhibition of CCR5, Science, 306, 485-487.

Libert,F.,Cochaux,P., Beckman,G., Samson, M., Aksenova,M., Cao,A., Czeizel,A., Claustres,M., DelaRúa,C., Ferrari,M., Ferrec,C., Glover,G., Grinde,B., Güran,S., Kucinskas,V., Lavinha,J., Mercier,B., Ogur,G., Peltonen,L., Rosatelli,C., Schwartz,M., Spitsyn,V., Timar,L., Beckman,L., Parmentier, M., Vassart,G., (1998) The 5 mutation conferring protection against HIV-1 in Caucasian populations has a single and recent origin in Northeastern Europe, Oxford University Press Human Molecular Genetics, 7, 399–406

Lieberman-Blum, S., Fung, H., Bandres, J. (2008) Maraviroc: A CCR5-receptor Antagonist for the Treatment of HIV-1 Infection, Clinical therapeutics, 30, 1228-1250

Lin, P-F., Blair, W., Wang, T., Spicer, T., Guo, Q., Zhou, N., Gong, Y-F., Wang, H., Rose, R.,Yamanaka, G., Robinson, B., Li, C-B., Fridell, R., Deminie, C., Demers, G., Yang, Z., Zadjura, L., Meanwhile N., Colonno, R. (2003) A small molecule HIV-1 inhibitor that targets the HIV-1 envelope and inhibits CD4 receptor binding, PNAS,100,no.19,11013-11018.

Liu, J., Barteshagi ,A.,Borgnia, M., Sapiro, G., Subramanian, S. (2008) Molecular architecture of native HIV-1 gp120 trimers. Nature, 455, 109-114

Meanwell, N., Kadow, J., (2003) Inhibitors of the entry of HIV into host cells, Current Opinion in Drug Discovery & Development, 6,451-461.

Melikyan, G. (2008) Common principles and intermediates of viral protein-mediated fusion: The HIV-1 paradigm, Retrovirology,5, 111-122.

Moyle, G. (2003) Stopping HIV fusion with enfuvirtide: the first step to extracellular HAART, Journal of antimicrobial Chemotherapy,51,213-217

Nardese, V., Longhi, R., Polo, S., Sironi, F., Arcelloni, C., Paroni, R., DeSantis, C., Sarmientos, P, Rizzi, M., Bolognesi, M., Pavone, V., Lusso, P. (2001) Structural determinants of CCR5 recognition and HIV-1 blockade in RANTES, Nature Structural Biology,8,611-615.

Nelson, P., Kim, H., Manning, W., Goralski, T., Krensky, A., (1993) Genomic organization and transcriptional regulation of the RANTES chemokine gene, Journal of Immunology, 151, 2601-2612

Nishiyama, Y., Murakami, T., Shikama, T., Kurita K., Yamamoto N. (2002) Anti-HIV-1 Peptides Derived from Partial Amino Acid Sequences of CC-Chemokine RANTES, Bioorganic & Medicinal Chemistry,10,4113–4117

Oppermann, M. (2004) Chemokine receptor CCR5: insights into structure, function, and regulation. Cellular Signalling, 16, 1201-1210

Pla, I., Damsceno, L., Vannelli, T., Ritter, G., Batt, C., Shuler, M., (2006) Evaluation o Mut+ and Muts Pichia pastoris for high level extracellular scFv expression under feedback control of the methanol concentration, Biotechnology progress, 22, 881-888.

Rizzuto, D., Wyatt, R., Hernandez-Ramos, N.,Sun,Y., Kwong, P.,Hendrickson, W., Sodroski, J. (1998) A conserved HIV gp120 Glycoprotein Structure Involved in Chemokine Receptor Binding. Science. 280, 1949-1953.

Rusconi, S., Moonis, M., Merrill, D., Pallai, P., Neidhardt, E., Singh, S., Willis, K., Osburne, M., Profy, A., Jenson, J., Hirsch, M., (1996) Naphthalene sulfonate polymers with CD4-Bloking and Anti-Human Immunodeficiency Virus Type 1 Activities, Antimicrobial Agents and Chemotherapy, 40,234-236.

Samson, M., Libert, F., Doranz, B., Rucker, J., Liesnard, C., Farber, C., Saragosti, S., Lapoumeroulie, C., Cognaux, J., Forceille, C., Muldermans, G., Verhofstede, C., Burtonboy, G., Georges, M., Imai, T., Rana, C., Doms, R., Vassart, G., Parmentier, M. (1996) Resistance to HIV-1 infection in Caucasian individuals bearing mutant allelesof the CCR-5 chemokine receptor gene, Nature,382,722-725.

Simmons, G., Clapham, P., Picard, L., Offord, R., Rosenkilde, M., Schwartz, T., Buser, R., Wells, T., Proudfoot, A. (1997) Potent Inhibition of HIV-1 infectivity in macrophages and lymphocytes by a novel CCR5 antagonist, Science, 276,276-279.

Skelton, N., Aspiras, F., Ogez, J., Schall, T. (1995) Proton NMR Assignments and Solution Conformation of RANTES, a Chemokine of C-C type, Biochemestry,34.5329-5342.

Song A., Chen, Y., Thamatrakoln, K., Storm, T., Krensky, A. (1999) RFLAT-1: A new zinc finger transcription factor that activates RANTES gene expression in T lymphocytes, Immunity,10,93-103

Song, A., Nikolcheva, T., Krensky, A. (2000) Transcriptional regulation of RANTES expression in T lymphocytes, Immunological Reviews,177,236-245.

Welch, B., VanDemark, A., Heroux, A., Hill, C., Kay, M., (2007) Potent D-peptide inhibitors of HIV-1 entry. ProcNatlAcadSci USA,104,16828-16833.

Wilen, C., Tilton, J., Doms, R., (2012) Molecular Mechanisms oh HIV entry.Advances in Experimental Medicine and Biology. 726, 223-242

Wong, P., Wyatt, R., Robinson, J., Sweet, R., Sodroski, J., Hendrickson, W., (1998) Structure of an HIV gp120 envelope glycoprotein in complex with the CD4 receptor and a neutralizing human antibody. Nature 393, 648-659.

Wu, H., Myszka, D., Tendian, S., Brouillette, C., Sweet, R., Chaiken, I., Hendrickson, W., (1996) Kinetic and structural analysis of the CD4 receptors that are defective in HIV gp120 binding.ProcNatlAcadSci USA. 93, 15030-15035

CHAPTER II

CELL LINE CONSTRUCTION AND FERMENTATION DEVELOPMENT

Abstract

Pichia pastoris is a well know microorganism that has the ability to express extra and intracellular recombinant proteins. *Pichia pastoris* has a large amount of genotype strains that are derived from the wild-type strain Y-11430. The X-33 is also a wild-type strain that have the capability to accept recombinant gene. A great variety of expression vectors for *P. pastoris* enables the facile development of multiple clonal linages containing the recombinant gene. Using a yeast shuttle vector one can select clones that can express the protein of interest from those who are not capable of expression. The presence of the alcohol oxidase enzyme (AOX) in the genomic information of the yeast *Pichia pastoris* is particularly beneficial for selection and induction of cells that produce the protein of interest. The AOX enzyme allows the usage of methanol as the sole carbon source for the production of biomass and energy metabolism. The expression of protein and posterior translocation depends in the particular features of some shuttle vectors. For example, the pPICZαA vector has the ability to secrete the protein of interest out of the cell into the fermentation broth. Secretion is achieved by the addition of the α-leading factor transcriptional unit. The leading factor is removed in the Golgi apparatus by enzymatic action of the KEX2 protease that allows the secretion of the protein of interest. In this research, The X-33 wild type is used as host microorganism for the vector pPICZαA–5P12-Rantes.

The fermentation development focused in both the determination of the maximum growth rate and the establishment of a relation between the methanol growth rate and the methanol feed rate. The rate of growth was determined to be 0.0807 h^{-1} using methanol as sole carbon source. The equation $\nu_{MeOH} = 0.7573\ (\mu_{MeOH}) + 0.0024$ relates the methanol feed rate with the methanol growth rate.

Introduction

Pichia pastoris as a suitable system for heterologous protein expression

Pichia pastoris, recently reassigned to its genus *Komagataella pastoris* (*P. pastoris*) (Kurtzman et al, 2009), has been largely used for recombinant protein production. (Cregg et al, 2009). The *P. pastoris* system has the potential to express correctly folded proteins, grow at large cell density, use methanol as sole carbon source, and produce large amounts of protein using the alcohol oxidase (AOX) promoter that drives the gene expression of the desired protein (Daly et al, 2005).

The formation of haploids during *P. pastoris* life cycle offers advantages for the isolation and phenotype characterization of mutants. Mating occurs on nitrogen limitations and diploid cells are formed. *P. pastoris* is by definition homothallic and after mating the resulting diploid products can be maintained in the state by shifting to a standard growth medium. In this context, *P. pastoris* life cycle enables genetic manipulation due to its stability in the haploid state (Cregg et al, 1998).

P. pastoris offer a great variety of strains that can facilitate and enhance the production of recombinant proteins. For example, the wild type strain, X-33, is a positive methanol utilization strain. The strain GS115 is defective in the histidine dehydrogenase

gene (his4), and its use allows transformants to be selected based on the ability to grow in non-histidine containing media. The strain KM71 is a strain which chromosomal Alcohol Oxidase 1 (AOX1) has been deleted. KM71 uses a weaker promoter alcohol oxidase 2 (AOX2) that metabolize methanol in a lower rate than AOX1. Some other strains have a lower grade of vacuolar proteases that can degrade protein especially during high density cell fermentation. SMD1165 and SMD1163 are defective in vacuolar proteases and may help to reduce protein degradation (Higgins et al, 1998. Daly et al, 2005).

Expression vectors for *P. pastoris* have both common and specialized features. All vectors contain an expression cassette which is composed of a promoter sequence (commonly AOX1 promoter), multiple cloning sites for gene insertion and a transcriptional termination sequence that allows efficient polyadenylation (Li et al,2007). However, the most important feature is that all *E. coli* / *P. pastoris* shuttle vectors contain an origin of replication for plasmid maintenance. These vectors also have functional markers that make them usable for marker selection in both organisms (Cereghino et al, 2007). Specialized vectors are selected according to the expression requirements. For example, there are vectors that favor intracellular expression, some that favor extracellular secretion, some that offer different selectable markers or antibiotic resistance, and some that use promoters other than AOX1 (Higgins, Busser et al, 1998, Cereghino et al 2007). In this context, the vector pPICZαA induces extracellular protein secretion using the alpha mating factor (α-MF) secretion signal. This vector uses zeocin as antibiotic marker and allows plasmid integration to the AOX1 locus. These characteristics make this vector an optimal option when extracellular expression is required (Siren et al, 2006).

The glyceraldehyde 3-phosphate dehydrogenase (GAP) and AOX1 promoter are the more useful promoters during heterologous protein expression. The GAP promoter allows strong constitutive expression using either glucose or glycerol. However, the GAP promoter activity in cells grown in glycerol is two-thirds of the level observed for glucose (Cereghino et al, 2000). However, GAP promoter induce the production of acetate and ethanol than may be harmful to the protein of interest (Li et al, 2007).

The AOX1 promoter is used to drive the expression of recombinant proteins to high levels using methanol as sole carbon source (Daly et al, 2005). When AOX1 enzyme represents the 30% of the total protein content, AOX1 production may be induced by switching carbon source from glycerol to methanol. However, the importance of using AOX1 as a drive promoter resides in its functionality to metabolize large amounts of methanol to produce for both production of cell material and metabolism (Bollok et al, 2009).

Alcohol Oxidase (AOX) is the first enzyme that acts on the metabolic pathway of methanol. AOX is an oligomericflavoprotein that contains the flavin adenine dinucleotide (FAD) and the modified flavin adenine dinucleotide (mFAD). These flavoproteins are non-covalently attached to AOX to accomplish electron transfer (Bystrykh et al, 1991. Daly et al, 2005). *P. pastoris* has two genes that code for the alcohol oxidase enzyme: alcohol oxidase 1 (AOX1) and the alcohol oxidase 2 (AOX2). The AOX1 is responsible for at least 90% of the AOX activity, and AOX2 accounts for the rest (Pla et al, 2006). AOX is sequestered within the peroxisome along with catalase. AOX oxidizes methanol to formaldehyde and hydrogen peroxide that it is degraded by catalase (Figure 2.1). A portion of the produced formaldehyde leaves the peroxisome and is further oxidized to

formate and carbon dioxide by cytoplasmic dehydrogenases. These last reactions are the source of energy for cells growing on methanol. (Cereghino et al, 2000)

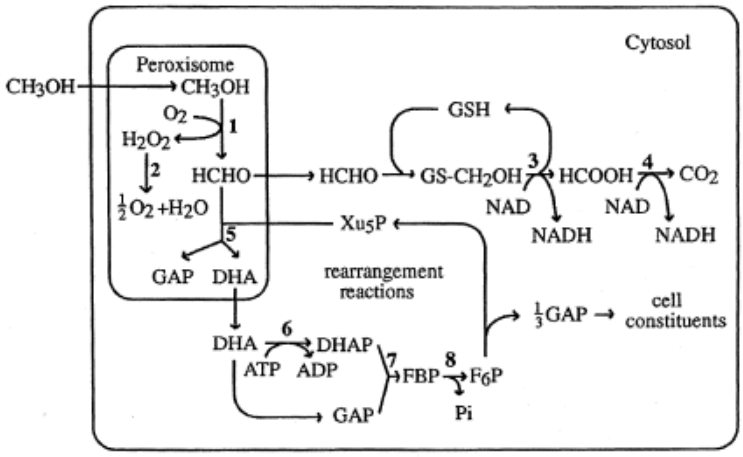

Figure 2.1. The methanol pathway in *P. pastoris*. 1 alcohol oxidase; 2 catalase; 3 formaldehyde dehydrogenase; 4 formate dehydrogenase; 5 dihydroxyacetone synthase; 6 dihydroxyacetone kinase; 7 fructose 1,6-biophosphate aldolase; 8 fructose 1,6-biphosphatase.

P. pastoris phenotypes are selected on the capacity to metabolize methanol: methanol utilization positive (Mut^+), Methanol utilization slow (Mut^s) and Methanol utilization negative (Mut^-). These phenotypes are the possible outcomes that can result after homologous recombination in the AOX1 promoter (Daly et al, 2005). Transformants with Mut^+ can synthesize large amounts of methanol due to the expression of AOX1. Mut^s transformants can processes low quantities of methanol mainly caused by the deletion of the AOX1 and expression of the weaker enzyme AOX2. Mut^- phenotypes contain neither AOX1 nor AOX2 in its genome (Pla et al, 2006).

P. pastoris allows high levels of recombinant protein expression due to its ability to reproduce and maintain high-cell densities during fermentation (Inan, et al 1999). Fermentation process can be subdivided in four operative sections. First, the batch phase in which *P. pastoris* grows freely using a salt medium with a non-fermentable carbon source like glycerol. Second, the fed-batch phase is mainly characterized for the growth under glycerol grow-limiting rate. Under this phase sub-products produced during batch phase like ethanol are used by the yeast, making them ready for the use of methanol (Zhang et al, 2000). Third, the transition phase characterized for a first injection of methanol and a constant reduction of the glycerol feed rate for three hours. This phase is of particular interesting because it defines the time zero for induction (Zhang, et al 2000). Finally, the methanol induction phase in which the carbon source is fed at growth limiting rate to avoid any prejudicial accumulation that may affect the cell. The induction phase activates the expression of the protein of interest (Cereghino et al, 2000).

Material and Methods

DNA Sequence construction, transformation and multiple inserts screening

5P12-Rantes DNA sequence was obtained from The Mintaka Medical Research Foundation trough the Biological Process Development Facility (BPDF) at University of Nebraska – Lincoln (UNL). The DNA sequence was synthesized by Gene Script and inserted in the pUC57 vector. The pUC57 containing the 5P12-Rantes gene was subcloned into *E. coli* DH5α strain. The *E. coli* DH5α–pUC57–5P12-Rantes strain was plated in Lb agar plate containing 100 mg/L ampicillin. Then, the pUC57–5P12-Rantes vector was extracted and purified as instructed in the DNA qiagen Miniprep kit. The

purified vector was digested with restriction enzymes Not I and Xho I. The digested solution is separated using agar gel. The DNA sequence that corresponds to the 5P12-Rantes was extracted from the gel and then purified. The purified 5P12-Rantes sequence is inserted into a previously digested pPICZαA vector and sub cloned into *E. coli* DH10B strain. Purified DNA sequence was shipped for sequence confirmation. Finally, the *E. coli* DH10B strain containing the pPICZαA–5P12-Rantes sequence was plated in Lb agarose gel with 5µg/L zeocin. 10 mL Lb broth is inoculated with 1µg of a well round shape form colony. The Lb broth is incubated at 37°C and 200 rpm for 10 hours. 1.5 ml of the resulting broth was treated as indicated in the Qiagen Miniprep Kit and later digested with PmeI enzyme for DNA linearization.

P. pastoris wild type X-33 is used as the hosting microorganism. Fresh competent cells are used for electroporation (Wu, et al 2004). Finally, *P. pastoris* transformation is completed by electroporation as indicated in section of transformation in the Pichia pastoris protocols (1998). The solution containing the transformants is plated in YSDS agar plates containing 100, 200, 500, 1000 and 1500 µg/mL zeocin. Colonies started to appear after 3 days of incubation at 30°C.

Table 2.1: X-33 amplification in YSDS/zeocin agar plates

YSDS/ Zeocin concentration	Colonies
100 µg/mL	25
200 µg/mL	16
500 µg/mL	6
1000 µg/mL	2
1500 µg/mL	0

Mut+ phenotype selection

Phenotype selection of the transformants is performed to discriminate strains with AOX activity from those whose AOX sequence has been deleted. A number is assigned to the each colony that grows in the YSDS plates. Each colony is transferred from the YSDS plate to Minimal Dextrose (MD) agar plate and the same colony is used to inoculate Minimal Methanol (MM) agar plates. Plates were incubated at 30°C and checked for colony formation every 24 hours. 3 colonies grew after 35 hours of inoculation. The colonies with the assigned number 8, 30 and 32 were chosen for further processing. This selection was based in the high zeocin resistance assuming that higher resistance is an indication of multiple sequence insert. The selected clones are assumed to have a better capability to metabolize methanol. All colonies grew after 48 hours of incubation however this indicates a slow tendency to metabolize methanol.

Table 2.2: Clones with high zeocin resistance

Colony Number	Zeocin Resistance
8	500 µg/mL
30	200 µg/mL
32	200 µg/mL

Selection of the clone is completed by running 3 fermentation batches using Basal Salts Medium (BSM**)**. Each batch ran at 1g/L methanol saturation in which clone number 8 showed to have a better capability to metabolize methanol as carbon source. Even though, clones number 30 and 32 have zeocin resistance both have demonstrated

methanol accumulation during fermentation reaching about 700 and 1300 ppm of methanol accumulated in the vessel during induction phase.

Fermentation Development

Fermentations were developed using 3 5-liter Bioflo III fermentor interfaced with the computer base software AFS – Biocommand32 (New Brunswick Scientific Co. Edison, GA). The outlet gas was diverted into two lines. The first line was directed to monitor the methanol concentration in the fermentation broth using a MC-168 methanol concentration monitor and controller (PTI instruments, Inc., Kathleen, GA). The second line was derived to a process mass spectrometer for on-line fermentation gas analysis (PrimaδB VGgas Thermo-Fisher Scientific) The AFS-Biocommand32 interface was used to monitor and control a peristaltic pump used for methanol feed (Model 101U/R, Watson-Marlon Ltd. England), scale (Model PG 12001-S, Mettler Todelo, Switzerland), and the methanol concentration monitor and control.

The main objective of the fermentation development process, using *P. pastoris* as host, is to obtain a high protein production level with a low methanol accumulation and high cell density. Fermentation process may be subdivided in four sections: Batch phase, glycerol fed batch phase, transition phase and induction phase.

The fermentors were inoculated with 100 ml of BMGY incubated for about 19 hours with 1 mL of stock culture at 30°C and 250 rpm shaking rate. Once the optical density at 600 nm (OD_{600}) reached a value between 8 and 10 the shake flask was stopped and aseptically 100 mL was transferred to each fermentor.

Each fermentation batch used 2L of BSM. Before inoculation, 8.7 ml of PTM1 salts and 2 mL of 5%v/v antifoam were injected directly to the vessel. The fermentation medium pH was adjusted to 5 with 20–30% ammonium hydroxide. The temperature was set up to 30°C and dissolved oxygen to 40%. Agitation was initially at 400 revolutions per minute (rpm) and set up in cascade response so the agitation will increase to maintain dissolved oxygen (DO) at 40%. These conditions are maintained until all the initial glycerol contained in BSM is consumed.

The fermentation batch phase has the objective to generate biomass prior to the production of protein. Glycerol, included in BSM, is used as the sole carbon source in the phase and the microorganism grows at non-limiting carbon supply. The table 2.3 provides information about the data extracted from this phase. Since the glycerol concentration in BMS is the same for all runs the results showed have little variability.

Table 2.3: Data from fermentation batch phase for a total of 20 experiments

Variable	Range
Batch phase specific growth rate	0.1766 - 0.1769 h^{-1}
Cell mass produced	98 – 100 g wet cells/L
Glycerol yield	2.45 – 2.5 g wet cells/g glycerol

The depletion of glycerol in BSM is characterized by a rapid increment in the DO value that is also known as DO spike which indicates the culmination of the batch phase (Inan et al 1999). During the glycerol fed-batch phase, a solution of 63% weight/volume (w/v) glycerol with 12 mL/L PTM1 salts is fed to the fermentation broth at 20

gr/Liter/hour feed rate (Zhang, 2000). During this phase all the sub-products (ethanol, acetate) produced in the batch phase are used for cell maintenance and growth (Zhang, et al2000). Glycerol fed-batch phase is completed after 1 hour of glycerol fed to obtain about 120 to 125 g wet cell/L.

Transition phase starts after 1 hour of glycerol feed. 1 g MeOH/L (1.26 mL/L) broth is injected into the fermentor and marks the time zero for induction. The glycerol feed rate is decreased from 20 g/L/h to 0 g/L/h over 3 hours. The mass spectrometer shows an increase in the methanol concentration in the fermentor after the first injection. The concentration of methanol decreases over time indicating the capability of cells to metabolize methanol. The transition phase is particularly important due to the gentle switch from glycerol to methanol will improve the cell ability to metabolize methanol (Zhang, et al 2000).

Methanol fed-batch phase starts once the methanol concentration measured by the mass spectrometer has decreased about 50 ppm. Methanol feed profile is developed to estimate both maximum growth rate and optimal process conditions.

Maximum growth rate development

The maximum growth rate indicates the rate at which *P. pastoris* grows in a non-limiting carbon source environment. To obtain the maximum growth rate (μ_{max}), a fermentor was set up with 2L of BSM with 8.7 mL of PTM1 salts at pH 5.0. After DO spike, glycerol is fed at 40 g/h over 1 hour. 1 g MeOH/L was injected in the fermentor and the concentration was determined by the methanol sensor. The processed outcome was monitored with the AFS-Biocommand32 interface. 1g MeOH/L saturation is

indicated by a constant value in the Biocommand trend view. Once the methanol concentration decrease, a second injection is performed and methanol feed starts once the constant saturation value is reached. Methanol pump feed rate is controlled by the AFS-Biocommand32 interface to maintain 1g MeOH/L saturation value in the fermentor. The table 2.4 shows the values to determine the specific growth rate.

Table 2.4: Fermentation values for maximum growth rate determination

Induction time	Wet Cell Weight	Fermentor Volume	Biomass
5.60	135.4	2.05	277.57
11.01	190.2	2.23	424.146
12.98	215.3	2.32	449.496
14.00	232.3	2.37	550.551

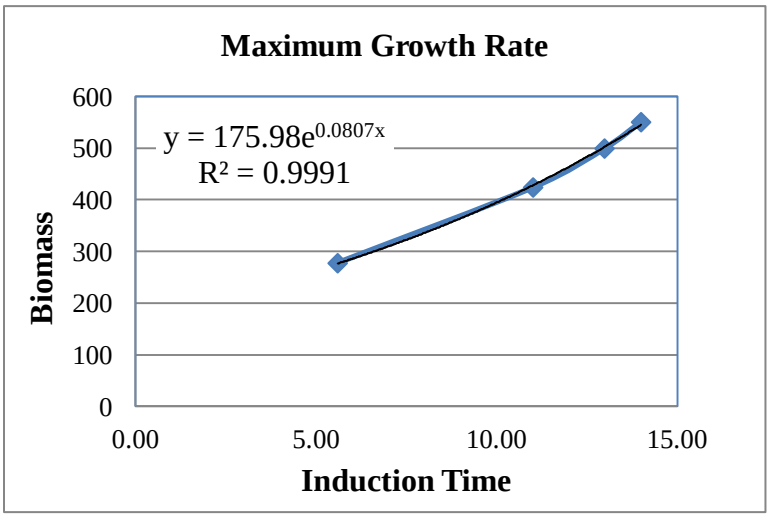

Figure 2.2 : Exponential regression to calculate maximum growth rate

The exponential regression shows that the specific growth rate has a value of 0.0807 h^{-1}.

Methanol Feed profile development

Methanol feed profile is developed to obtain an equation that will determine the relationship between the methanol consumption rate (ν_{MeOH}) and the growth rate during the methanol fed-batch phase (μ_{MeOH}). The growth rate will be limited by the amount of methanol fed during the methanol fed-batch phase. Four runs at different growth rates are performed. An equation proposed for methanol consumption rate (Sinha et al, 2003) is used as reference to determine the real relationship for this specific clone.

Table 2.5: Values for methanol consumption rate determination.

Fermentation	Proposed μ^*_{MeOH}	Real μ_{MeOH}	Real ν_{MeOH}
1	0.01	0.009	0.0099
2	0.025	0.0259	0.0225
3	0.04	0.0399	0.0302
4	0.06	0.0645	0.0524

The relationship between μ_{MeOH} and ν_{MeOH} is determined by linear regression with the calculated values (Zhang, et al 2000). The final equation is:

$$\nu_{MeOH} = 0.7573\ (\mu_{MeOH}) + 0.0024 \quad \text{(eq. 2.1)}$$

Results and Discussion

The development of *P. pastoris* growth rate and methanol consumption rate is important to the precise control of the amount of methanol fed during the methanol fed-batch phase. This information will allow to manage the methanol feed pump that ultimately is controlled by the AFS-Biocomand32 interface in which this data is entered.

Determination of the maximum growth rate for this specific clone is useful information towards the development of the fermentation process. The calculated value of 0.0807 h^{-1} was obtained at 1g/L methanol saturation in the fermentor vessel. Concentration higher than 3.75 g/L methanol saturation will have inhibitory effects on the specific growth rate (Zhang, et al 2000).

The equation proposed by Sihna et al 2000, was adjusted to the actual values that correspond to this specific clone. For all four fermentations, methanol was fed in a quasi-steady state condition at different exponential growth rates. This fermentation were performed below the inhibitory growth levels (Sihna, et al 2000). The actual equation (ν_{MeOH} = 0.7573 (μ_{MeOH}) + 0.0024) will be used in the experimental design for the exponential growth and exponential methanol feed rate.

References

Bollok, M., Resina, D., Valero, F., Ferrer, P. (2009) Recent patents on the Pichia pastoris expression system: Expanding the toolbox for recombinant protein production, Recent patents on biotechnology, 3, 192-201.

Cereghino, J., Cereghino, G. (2007) Vectors and strains for expression, Methods in Molecular Biology – Pichia protocols, 389, 11-25.

Cereghino, J., Cregg, J. (2000) Heterologous protein expression in the methylotrophic yeast Pichia pastoris, FEMS Microbiology reviews, 24, 45-66

Couderc, R., Baratti, J., (1980) Oxidation of methanol by the yeast Pichia pastoris purification and properties of the alcohol oxidase. Agricultural and biological chemistry,44(10), 2279-2289

Cregg, J., Chen, S., Johnsin, M., Waterham, H. (1998) Classical genetic manipulation, Methods in Molecular Biology – Pichia protocols, 103, 17-26.

Cregg, J., Russell, K.. (1998) Transformation, Methods in Molecular Biology – Pichia protocols, 103, 27-39.

Cregg, J., Tolstorukov, I., Kusari, A., Sunga, J., Madden, K., Chappell T. (2009) Expression in the Yeast Pichia pastoris, Methods in Enzymology, 463, 169-189.

Daly, R., Hearn, M. (2005) Expression of heterologous proteins in Pichia pastoris: a useful experimental tool in protein engineering and production. Journal of Molecular Recognition, 18, 119-138.

Higgins, D., Busser, K., Comiskey, J., Whittier, P., Purcell, T., Hoeffler, J., (1998) Small vectors for expression based on dominant drug resistance with direct multicopy selection, Methods in Molecular Biology – Pichia protocols, 103, 41-53.

Higgins, D., Cregg, J. (1998) Introduction to Pichia pastoris, Methods in Molecular Biology – Pichia protocols, 103, 1-16.

Jahic, M., Rotticci-Mulder, J., Martinelle, M., Hult K., Enfors, S-O., (2002) Modeling of growth and energy metabolism of Pichia pastoris producing a fusion protein, Bioprocess and biosystems engineering,24,385-393.

Jahic, M., Wallberg, F., Bollok, M., Garcia, P., Enfors, S-O (2003) Temperature limited fed-batch techniques for control of proteolysis in Pichia pastoris bioreactor cultures. Microbial cell factories, 2, 1-11

Kurtzman, C. (2009) Biotechnological strains of Komagataella (Pichia) pastoris are Komagataella phaffi as determined from multigene sequence analysis, Journal of Industrial Microbiology Biotechnology, 36, 1435-1438.

Li, P., Anumanthan, A., Gao, X., Ilangovan, K., Suzara, V., Düzgünes, N., Renugopalakrishan V. (2007) Expression of Recombinant Proteins in Pichia pastoris Applied Biochemestry Biotechnology, 142, 105-124.

Pla, I., Damsceno, L., Vannelli, T., Ritter, G., Batt, C., Shuler, M., (2006) Evaluation o Mut+ and Muts Pichia pastoris for high level extracellular scFv expression under feedback control of the methanol concentration, Biotechnology progress, 22, 881-888.

Sinha, J., Plantz, B., Zhang, W., Gouthro, M., Schlegel, V., Liu, C-P., Meagher, M., (2003) Improved production of recombinant ovine interferon-τ by Mut+ strain of Pichia pastoris using an optimized methanol feed profile. Biotechnology progress, 19, 794-802

Siren, N., Weegar, J., Dahlbacka, J., Kalkkinen, N., Fagervik, K., Leisola, M., Weymarn, N. (2006) Production of recombinant HIV-1 Nef (negative factor) protein using Pichia pastoris and low temperature fed-batch strategy, Biotechnology Applied Biochestry, 44,151-158

Sunga, A., Tolstorukov, I., Cregg, J., (2008) Posttranformational vector amplification in the yeast Pichia pastoris. FEMS yeast Res,8,870-876

Wu, S., Letchworth, G., (2004) High efficiency transformation by electroporation of Pichia pastoris pretreated wit lithium acetate and dithiothreitol, Biotechniques, 36, 152-154

Zhang, W., Bevins, M., Plantz, B., Smith, L., Meagher, M., (2000) Modeling Pichia pastoris Growth on Methanol and Optimizing the production of a recombinant protein, the heavy-chain fragment C of botulinum neurotoxin, serotype A. Biotechnology and bioengineering, 70,1-8.

Zhang, W., Liu, C-P, Inan, M., Meagher, M., (2004) Optimization of cell density and dilution rate in Pichia pastoris continuous fermentations for production of recombinant proteins, Journal Industrial Microbiology and Biotechnology, 31, 330-334.

CHAPTER III

RESPONSE SURFACE METHODOLOGY AND CENTRAL COMPOSITE DESIGN

ABSTRACT

Fermentation process development focuses upon the optimization of expression of a target molecule. The central composite design and the response surface methodology is a mathematical and statistical tool for evaluating the responses necessary to optimize a fermentation process (Dey et al 2001, Hao et al 2006). *P. pastoris* is frequently used for the production of recombinant heterologous proteins (Inan, et al 1999). However, there are many variables that may affect cell's productivity. These variables may include pH, temperature, Dissolve Oxygen, Agitation speed, medium composition, methanol growth rate and methanol feed rate (Inan et al 1999). This research is focused in the evaluation of the effect of temperature, pH and Methanol growth rate are evaluated in their effect on the total protein secretion, active protein secreted and Specific yield in the yeast *P. pastoris*.

The central composite design (CCD) is an experimental design used to allocate the operation variables into a range of evaluation. Temperature, pH and methanol growth rate are evaluated in a range defined by the CCD.

The response surface methodology (RSM) provides the statistical elements necessary for the evaluation of Temperature, pH and methanol growth rate. The RSM focused in the construction of geometrical models that can predict the behavior of the factors in the area of evaluation. In addition, the RSM enables the independent evaluation of each factor and their interaction within the proposed model.

INTRODUCTION

Response surface methodology (RSM) is a collection of mathematical and statistical methods to evaluate relationships between a group of quantitative independent variables and one or more responses. The RSM enables to evaluate operation variables that may or may not have significant effect in the main response (Myers 1976, Parampalli et al 2007, Inan et al 1999). The optimization of fermentation process is an important step in the development of feasible processes (Ghosalkar et al 2008). The fermentation process optimization implies the evaluation of medium composition, glycerol feed rate, methanol feed rate, temperature, pH, dissolve oxygen, air/oxygen flow rate and agitation speed (Inan, et al 1999). In this study, temperature, pH and methanol growth rate are evaluated to determine their effect in the total amount of 5P12-Rantes produced, the active 5P12-Rantes and the specific yield.

The central composite design, CCD, is used to build a second order experimental model (Myers, 1976). CCD is composed of a factorial design, a set of central points, and axial points equidistant to the center point.

The factorial design component of CCD is of the class 2^k factorial where k represents the number of relevant factors or variables. Each of the variables is taken at two levels meaning that each variable has a low and high numeric value. A coded numeric value of -1 and +1 is assigned to represent the variable's low and high values. The geometric representation of a factorial is a cube in which each corner represents an interaction of the factors. In this perspective, 8 interactions are to be evaluated when 3 processing variables are selected to determine their significance in the final response (Myers, 1976).

The axial component of CCD refers to the points that are equidistant from the center of the cube formed for the factorial design. A spherical design is obtained in the reason that there is an equal variance from the center to all the points in the sphere. In consequence, there is a positive axial value (+α) and a negative axial value (-α). The axial points add two more levels in each variable. The α value is calculated from the equation $\alpha = (n_i)^{1/4}$. Where, n_i represent the number of interactions obtained from the factorial design. Thus, for 8 interactions $\alpha = 1.682$ (Myers, 1976).

The central point component in the CCD is the average of the high and low values determined in the factorial design. The central point or zero point may be defined as the region where the optimal conditions are supposedly met. The addition of the central point in the design increases the level's design in one unit to a total of 5 levels for each variable.

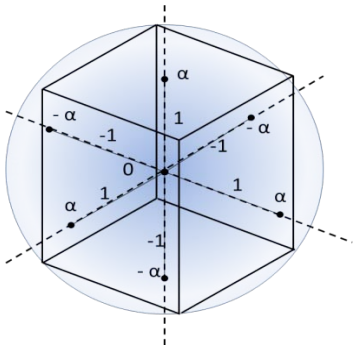

Figure 3.1. Layout of the Central Composite Design (CDD) for 3 variables at 5 levels

The RMS allows the introduction of blocks that facilitate the accomplishment of experiments. Blocking is justified based on the physical and time limitations to run experiments. However, blocking may have some effects over the final response. If the estimations of the independent and interaction effects of the selected variables are not

affected by blocking, the inclusion of blocks in the experimental design is justified (Myers, 1976).

The selection of variables for the analysis using RSM is completed in order to determine which factor may or may not have an important effect in the final response. Basic information about the protein sequence, pH stability, post transformational modifications will provide a better understanding of possible factors that can affect the protein production during fermentation.

GROWTH CONDITIONS

Methanol growth rate

The methanol growth rate is determined during the induction phase. The amount of methanol fed during this phase is calculated using equation 2.1. The methanol feed rate is established by values determined in the CCD. The methanol feed rate determines how fast the microorganism grow using this carbon source. However, there is an important link between the methanol feed rate and the amount of protein produced in the reactor vessel during the induction phase (Zhang, et al 2000). A lower methanol feed rate implies a slow growth rate and a slow protein production that could or could not be beneficial for the overall production. In other hand, a high methanol feed rate results in a rapid grow of the microorganism and an accelerated protein production that may be affected by the elevated methanol feed rate. (Sinha, et al 2003). Nevertheless high cell density is reached in the least amount of time and the accumulation of methanol in the fermentation vessel could be detrimental for the microorganism. (Sihna, et al 2003, Zhang et al 2000).

Temperature

Pichia pastoris generally uses temperature of 30°C (Wegner, US Patent 1983). However, the cell productivity may be affected by the temperature at which protein secretion is induced. Positive effects in production of heterologous recombinant protein have been reported when lowering temperature (Dragosits, et al 2008). Proteins tend to have more stability and proteases activity is decreased when fermentation is carry out at low temperatures. Nevertheless, low temperature during induction phase decrease the activity of the AOX enzyme and the tendency of accumulate methanol may have negative effects in the protein production. Temperatures ranging from 24°C to 30°C during the induction phase are preferably selected in order to evaluate their effect in the responses (Inan, et al 1999).

pH

Pichia pastoris has the ability to grow in a broader range of pH values. Expression of recombinant proteins were investigated in pH values from 3 to 7. The protein stability and activity is the main response to evaluated at different pH values (Inan et al 1999, Zhang et al 2000, Slininger et al 1990). The Acidity or alkalinity in which the process is run has an effect in both microorganism growth rate and protein production.

5P12-RANTES PROPERTIES

The 5P12-Rantes, an anti-HIV microbicide, has a molecular weight of 7.905 KDa and isoelectric point of 10.2. This protein was developed with the final intention to be used as a vaginal topical gel and prevent the spread of HIV infections disease. The acidic environment of the vagina (3.5 to 4.2) dictates the 5P2-Rantes stability and activity under

this condition (Gaertner, et al 2008). The amino acid sequence of 5P12-Rantes was established after an exhaustive investigation in which the inclusion of a motif Q-G-P-P at the N-terminus (Figure 3.2) reveals a remarkable anti-HIV activity over the other candidates. The next five amino acids residues affect both anti HIV-potency and the capacity for receptor interaction (Gaertner, et al 2008). The complete 5P12-Rantes amino acid sequence has a total of 69 amino acid residues distributed as follow: Q G P P L M A T Q S C C F A Y I A R P L P R A H I K E Y F Y T S G K C S N P A V V F V T R K N R Q V C A N P E K K W V R E Y I N S L E M S

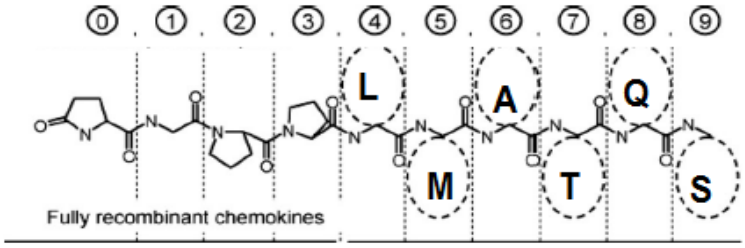

Figure 3.2: 5P12-Rantes sequence at the N terminal

The stability and activity of the 5P12-Rantes is limited by the spontaneous formation of a Pyro-glutamic residue at the N-terminal of the amino acid sequence and the formation of two disulfides bonds between the cysteine residues. The formation of the pyroglutamic acid (pyro-Q) enhances the protein stability, hydrophobicity and anti HIV-potency. In addition, the pyro-Q improves low intracellular sequestration and decrease the G protein-linked signaling activity (Gaertner, et al 2008). The N-terminal glutamine (Q) is converted into pyro-glutamic acid (pyro-Q) (Figure 3.3) (Dick, et al 2006). The two disulfide bonds occur between the cysteine residues at position 11 with 35 and 12 with 51 to form a G shape structure. The human Rantes structure has an analogous shape

to the 5P12-Rantes (Figure 3.4) (Burke-Gaffney et al 2002). The pyro-Q formation is an important post translational modification with effects in the functionality of the protein 5P12-Rantes. The formation of pyro-Q at the N-terminal protects the protein against proteolitic degradation (Kumar et al 2012).

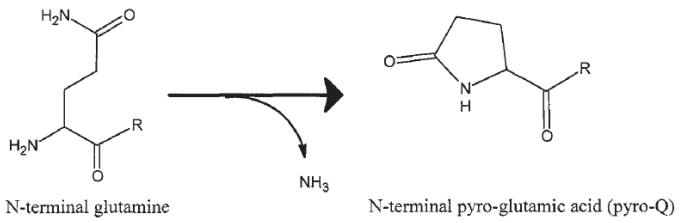

Figure 3.3: The conversion of glutamine to pyro-glutamic acid

The 5P12-Rantes stability and activity delimit the pH and temperature ranges of operation. However, the formation of the pyro-Q at the N-terminal during fermentation has not been investigated (Dick, et al 2006). Pyro-Q formation is induced by the increase of temperature in a non-enzymatic reaction. (Kumar et al, 2012)

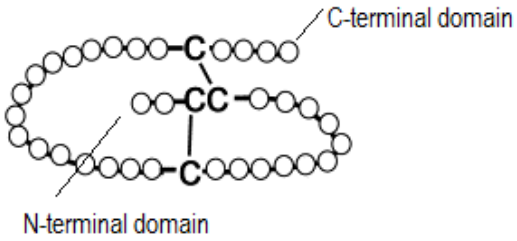

Figure 3.4: Human Rantes G shape with 2 disulfide bonds. The chemotaxis effect depends of the formation of the G-shape.

Transformation of the un-cyclized form to cyclized is achieved by heating up purified 512-Rantes solution at 60°C, pH 6.0 and 100mM potassium phosphate. Even though this purification step maximizes the conversion of un-cyclized 5P12-Rantes, the usage of chemicals and energy increase the cost of downstream processing.

MATERIAL AND METHODS

Central composite design

A second order design composed of 3 blocks. 3 factors at 5 levels CCD was used to investigate the effect of methanol growth rate, temperature and pH in the production of 5P12-Rantes, 5P12-Rantes activity and specific yield. The CCD comprises a total of 20 experiments: a full factorial design (8 experiments), 6 axial points, and 6 central points. 3 blocks were used to subdivide the experiments in three groups. 4 factorial points with 2 central points for the first two blocks and the third one comprise 6 axial points with 2 central points. Each block represents a bioreactor and 2 central points are proposed to estimate the error for each bioreactor.

Table 3.1: 3 factors at 5 levels estimated values

Factor	Axial (-α)	Low (-1)	Normal (0)	High (+1)	Axial (+α)
Methanol growth rate ($MeOH_{GR}$) h^{-1}	0.010	0.016	0.025	0.0339	0.040
Temperature (T) °C	24.06	25.25	27.00	28.75	29.94
pH	1.98	2.50	3.25	4.00	4.51

Table 3.2: CCD matrix for 3 factor 5 level 3 blocks

Block	Coded Values			Un coded values			Lot Number
	MeOH (X_1)	Temp (X_2)	pH (X_3)	MeOH	Temp	pH	
1	-1	-1	-1	0.0161	25.25	2.50	MK-GR- 11
1	+1	+1	-1	0.0339	28.75	2.50	MK-GR- 05
1	+1	-1	+1	0.0339	25.25	4.00	MK-GR- 13
1	-1	+1	+1	0.0161	28.75	4.00	MK-GR- 08
1	0	0	0	0.0250	27.00	3.25	MK-GR- 16
1	0	0	0	0.0250	27.00	3.25	MK-GR-17
2	+1	-1	-1	0.0339	25.25	2.50	MK-GR-20
2	-1	+1	-1	0.0161	28.75	2.50	MK-GR-10
2	-1	-1	+1	0.0161	25.25	4.00	MK-GR- 07
2	+1	+1	+1	0.0339	28.75	4.00	MK-GR- 14
2	0	0	0	0.0250	27.00	3.25	MK-GR-18
2	0	0	0	0.0250	27.00	3.25	MK-GR-21
3	-1.682	0	0	0.0100	27.00	3.25	MK-GR-02
3	+1.682	0	0	0.0400	27.00	3.25	MK-GR-04
3	0	-1.682	0	0.0250	24.06	3.25	MK-GR-12
3	0	+1.682	0	0.0250	29.94	3.25	MK-GR-09
3	0	0	-1.682	0.0250	27.00	1.99	MK-GR-06
3	0	0	+1.682	0.0250	27.00	4.51	MK-GR-15
3	0	0	0	0.0250	27.00	3.25	MK-GR-22
3	0	0	0	0.0250	27.00	3.25	MK-GR-01

Dry cell weight

Dry cell weight, DCW, is determined using a correlation between the data obtained from the optical density at 600 nm (OD_{600}) and the DCW in g/L. The optical density is measured using a UV spectrometer cary 50. The Varian Cary 50 UV-VIS spectrometer is set up at a wavelength of 600 nm. This equipment allows accurate measurements when absorbance is determined between 0 and 1. In consequence, dilutions are performed in the original sample once high cell concentration is reached in the fermentor vessel. The dry cell weight (DCW) is calculated after washing the cell resulting from the wet cell weight (WCW) calculations. Then the tubes are dried at 80°C for 24 hours (Inan et al 1999, Kunert et al 2008). The final correlation between dry cell weight and OD_{600} is indicated in the following equation.

$$DCW\ (g/L) = 0.2547\ (OD_{600}) + 0.1902 \quad \text{(Eq. 3.1)}$$

The calculated DCW represents around 20% of the WCW for a total of 20 experiments. The DCW estimated values are to be used in the determination of the specific yield in the final response.

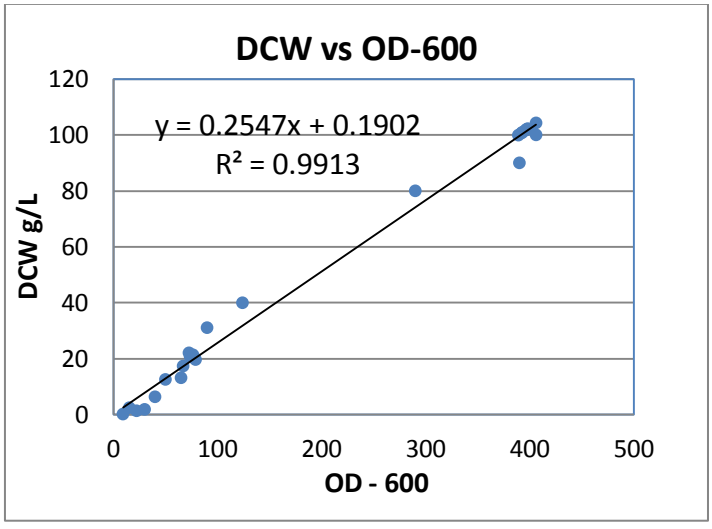

Figure 3.5: Linear regression to estimate relationship between DCW and OD_{600}.

5P12-Rantes protein essay

5P12-Rantes is analyzed at 280 nm of absorbance using high performance liquid chromatography (HPLC-Waters). A strong cation-exchange (SCX) column is used to perform the analysis (PolySulfoEthyl A^{TM}, 100x4.6mm, 5 µm, 300Å, PolyLC Inc. 104SE0503). The buffer solutions for this analysis are Mobile phase A: 50nM 2-(N-morpholino)ethanesulfonic acid (MES) at pH 6.4, Mobile phase B: 50nM MES and 1M Sodium Chloride (NaCl) at pH 6.4, Mobile phase C: 0.45 µm filtered water and Mobile phase 40mM Ethylenediaminetetraacetic acid (EDTA).

The HPLC passivation procedure is achieved by rinsing the installed column with mobile phase C and then mobile phase D at 0.1mL/min and 1.0 mL/m respectively. After passivation the column is rinsed with mobile phase B at 0.5ml/L and then mobile phase A at 1.0 mL/min.

The SCX column is heated up to 40°C and then each sample is loaded in the system. The table 3.3 shows the gradient used in the HPLC system.

Table 3.3: HPLC mobile phase gradient

Step	Time (minutes)	Flow (mL/m)	% A	% B
1	0	1.0	100.0	0.0
2	2.0	1.0	100.0	0.0
3	8.0	1.0	70.0	30.0
4	40.0	1.0	45.0	55.0
5	43.0	1.0	0	100.0
6	45.0	1.0	100.0	0.0
7	50.0	1.0	100.0	0.0

5P12-Rantes is eluted in the 16 and 19 minute range (Figure 3.6). Two different retention time reflex the existence of two forms of the protein. The 5P12-Rantes with pyroglutamic acid (cyclized form) at the N-terminal is eluted at 16 minutes. Meanwhile, the form with glutamine (un-cyclized form) at the N-terminal is eluted at 19 minutes. The total concentration of 5P12-Rantes is a result of the sum of the peak area of both cyclized and un-cyclized form.

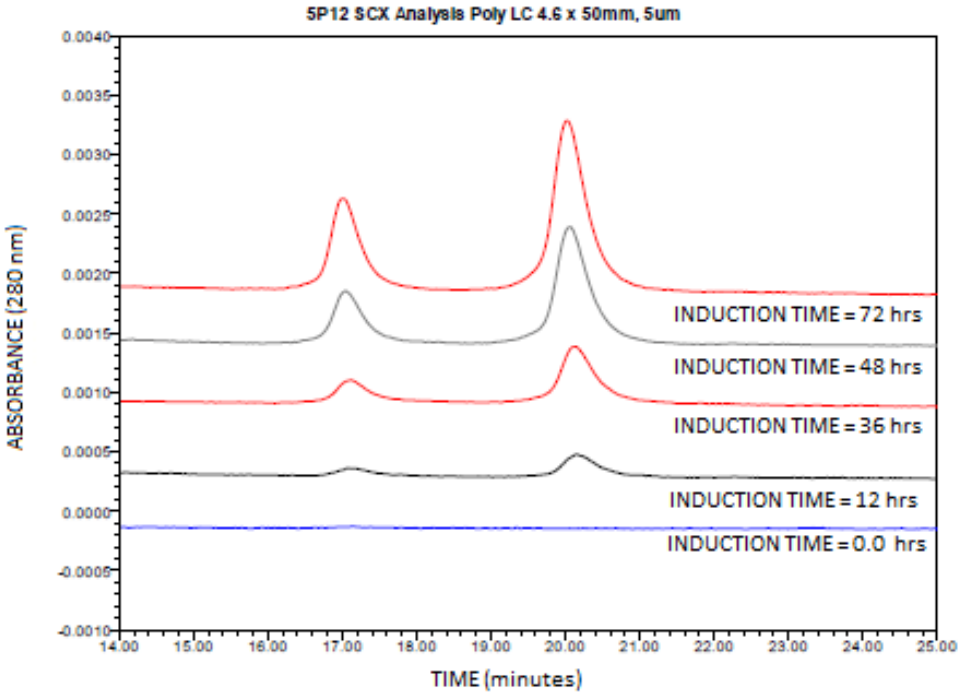

Figure 3.6: Chromatogram for quantitative analysis of 5P12-RANTES at different times during the methanol fed-bath phase

Specific Yield

The Specific yield represents the ratio of the total amount of 5P12-Rantes produced by each batch and the dry cell weight at the end of fermentation. The specific yield provides the experimenter information about the efficiency of the cell in producing both cyclized and un-cyclized 5P12-Rantes.

Results and Discussion

Table 3.4 shows the results of the responses: The total 5P12-Rantes, the active form of 5P12-Rantes and the Specific yield. The first response represents the sum of the active and inactive form of 5P12-Rantes produced during fermentation. The active form of the protein represents the concentration of cyclized 5P12-RANTES in the fermentation broth. The specific yield is another way to measure the efficiency of the overall process.

Table 3.5 shows the runs at which the production of 5P12-Rantes is maximized. These values correspond to the runs performed at the zero point.

Table 3.6 shows the conditions at which the maximum concentration of active 5P12-Rantes is achieved. This result shows that temperature has a important effect over the formation of pyro-glutamic acid.

Even though these results shows some predictability of the responses doesn't provide, by themselves, a model in which interpolation of the variables can be performed. The models for prediction of responses are to be evaluated using the response surface methodology and the central composite design. These statistical tools will provide equations that can be adjusted to the quantitative analysis and determine their accuracy and precision.

Table 3.4: Analytical results using SCX column

Lot Number	Total 5P12-Rantes mg/L	Active 5P12-Rantes mg/L	Specific Yield mg Total 5P12-Rantes / g Dry cell
MK-GR- 11	40.60	17.92	0.1185
MK-GR- 05	26.20	12.98	0.0860
MK-GR- 13	34.85	10.13	0.0881
MK-GR- 08	3.54	2.13	0.0102
MK-GR- 16	55.14	29.03	0.1570
MK-GR- 17	53.53	23.96	0.1542
MK-GR- 20	22.43	12.50	0.0654
MK-GR- 10	39.53	30.32	0.1104
MK-GR- 07	21.80	3.98	0.0685
MK-GR- 14	27.19	7.55	0.0668
MK-GR- 18	57.08	24.49	0.1621
MK-GR- 21	56.29	26.10	0.1524
MK-GR- 02	22.15	9.44	0.0796
MK-GR- 04	48.64	19.05	0.1286
MK-GR- 12	2.12	0.84	0.0062
MK-GR- 09	32.08	14.86	0.0989
MK-GR- 06	0.27	0.10	0.0110
MK-GR- 15	0.30	0.03	0.0008
MK-GR- 22	55.81	26.35	0.1496
MK-GR- 01	56.42	26.91	0.1735

Table 3.5: Experiments with high 5P12-Rantes concentration

Block	MeOH X_1	Temp X_2	pH X_3	MeOH	Temp	pH	Id Number	5P12-Rantes (mg/L)
1	0	0	0	0.0250	27.00	3.25	MK-GR- 16	55.14
1	0	0	0	0.0250	27.00	3.25	MK-GR- 17	53.53
2	0	0	0	0.0250	27.00	3.25	MK-GR- 18	57.08
2	0	0	0	0.0250	27.00	3.25	MK-GR- 21	56.29
3	0	0	0	0.0250	27.00	3.25	MK-GR- 22	55.81
3	0	0	0	0.0250	27.00	3.25	MK-GR- 01	56.42

Table 3.6: Highest production of active 5P12-Rantes

Block	MeOH X1	Temp X2	pH X3	MeOH	Temp	pH	Id Number	5P12-Rantes (mg/L)
2	-1	+1	-1	0.0161	28.75	2.50	MK-GR-10	30.32

References

Burke-Gaffney, A., Brooks, A., Bogle, R. (2002) Regulation of chemokine expression in atherosclerosis, Vascular pharmacology, 38, 283-292

Dey, G., Mitra, A., Banerjee, R., Maiti, B., (2001) Enhanced production of amylase by optimization of nutritional constituents using response surface methodology, Biochemical Engineering Journal, 7,227-231.

Dick, L., Kim, C., Qiu, D., Cheng, K-C., (2006) Determination of the origin of the N-terminal Pyro-glutamate variation in monoclonal antibodies using model peptides, Biotechnology and Bioengineering, 97, 544-553.

Dragosits, M., Stadlmann, J., Albiol, J., Baumann, K., Maurer, M., Gasser, B., Sauer, M. Altmann, F., Ferrer, P., Mattanovich, D., (2008) The effect of temperature on the proteome of recombinant Pichia pastoris, Journal of proteome research, 8, 1380-1392.

Gaertner, H., Cerini, F., Escola, J., Kuenzi, G., Melotti, A., Offord, R., Rossito-Borlat, I., Nedellec, R., Slkowitz, J., Gorochov,G., Moiser, D., Hartley, O., (2008) Highly potent, fully recombinant anti-HIV chemokines: Reenginering a low cost microbicide. PNAS, 105, 17706-17711

Ghosalkar, A., Sahai, V., Srivastava, A. (2008) Optimization of chemically defined médium for recombinant Pichia pastoris for biomass producción, Bioresource technology, 99, 7906 – 7910.

Hao, X-C., Yu, X-B., Yan, Z-L., (2006) Optimization of the medium for the production of cellulose by the mutant trichoderma reesei WX-112 Using Response Surface Methodology. Food Technology and Biotechnology, 44, 89-94.

Inan, M., Chiruvolu, V., Eskridge, K., Vlasuk, G., Dickerson, K., Brown, S., Meagher, M., (1999) Optimization of temperature-glycerol-pH conditions for a feed-batch fermentation process for recombinant hookworm (Ancylostoma caninum) anticoagulant peptide (AcAP-5) production by Pichia pastoris, Enzyme and Microbial Technology, 24, 438-435.

Kumar, A., Bachhawat, A., (2012) Pyroglutamic acid: throwing light on a lightly studied metabolite, Current Science, 102, 288-297

Kunert, R., Gach, J., Katinger, H., (2008) Expression of a Fab fragment in CHO and Pichia pastoris a comparative case study, BioProcess International, 6, 34 – 40.

Myers, R., Response Surface Methodology, Edwards Brothers, Ann Arbor, MI, 1976

Parampalli, A., Eskridge, K., Smith, L., Meagher, M., Mowry, M., Subramanian, A., (2007) Development of serum-free media in CHO-DG44 cells using a central composite statistical design. Cytothecnology,54,57-68

Sinha, J. Plantz, B., Zhang, W., Gouthro, V., Liu, C-P, Meager, M., (2003) Improved production of recombinant ovine interferon-τ by Mut+ strain of Pichia pastoris using and optimized methanol feed profile, Biotechnology Progress, 19, 794-802.

Slininger, P., Bothast, R., Ladish, M., Okos, M., (1990) Optmum pH and temperature conditions for xylose fermentation by Pichia stiptis, Biotechnology and Bioengineering,35, 727-731

Wegner, E., Biochemical conversions by yeast fermentation at high cell densities, 1983, U.S. Patents 4414329

Zhang, W., Bevins, M., Plantz, B., Smith, L., Meagher, M. (2000) Modeling Pichia pastoris growth on methanol optimizing the production of a recombinant protein, the heavy-chain fragment C of botulinum neurotoxin, serotype A, Biotechnology and Bioengineering, 70, 1-8.

Zhang, W., Inan, M., Meagher, M., (2000) Fermentation strategies for recombinant protein expression in the methylotrophic yeast Pichia pastoris, Biotechnology and Bioprocessing Engineering,5, 275-287

Zhang, W., Liu, C-P., Inan, M., Meagher, M., (2004) Optimization of cell density and dilution rate in Pichia pastoris continuous fermentation for production of recombinant proteins, Journal Industrial Microbiology and Biotechnology, 31, 330-334.

CHAPTER IV

CALCULATIONS AND ANALISIS OF VARIANCE

ABSTRACT

The analysis of variance (ANOVA) is a statistical test used in the analysis of experimental data. The CCD model describes the behavior of the production of 5P12-Rantes. This model is evaluated using analysis of variance. The ANOVA provides statistical tools to evaluate statistical hypotheses. In this context, the acceptance or rejection of the null hypothesis dictates the level of significance of each factor. Then, the alternative hypothesis is adopted if the null hypothesis is rejected (Walpole, 2007). The F-test is used to estimate the effect of each variable in the final response and whether or not the null hypothesis is rejected. The null hypothesis is rejected if the value of F-calculated (F-calc) is higher than the F-critical (F-crit). The rejection of the null hypothesis implies some level of significance of the factor in the final response. The P-value helps to discriminate between the factors that are significant from those which have not effect over the response. For example, a P-value lower than 0.05 indicates significance. The level of significance increases as the value approaches to zero. The F-test and the P-value evaluation determine the level of significance of each factor over a particular response. The acceptance or rejection of the proposed model will depend on the statistical analysis of the responses.

INTRODUCTION

The analysis of variance (ANOVA) is a statistical method used in the testing of statistical hypotheses. The statistical hypotheses are composed of the null hypothesis and the alternative hypothesis. The acceptance of rejection of the null hypothesis is based in the determination of value or F-calc. the F-calc represent ratio of the media square value of any factor and the residual error. The F-crit value is determined in the F-distribution probability table using the degrees of freedom of both numerator and denominator (Walpole, 2007). The calculation of P-value is used to evaluate the significance of each selected variable in the experiments. The standard value of 5% is chosen as standard value of significance for the evaluation of responses using ANOVA. The data obtained from the analytical analysis of the fermentation broth is used to perform the ANOVA using the software Minitab 16.

HYPOTHESES

The proposed equation to define the responses defines the effects of the selected variables ($MeOH_{GR}$, T, pH). To define the response equation, X_1, X_2 and X_3 are assigned to $MeOH_{GR}$, T, and pH respectively.

$$Y_{Total5P12\text{-}Rantes} = \mu_\beta + \beta_1X_1 + \beta_2X_2 + \beta_3X_3 + \beta_{11}X_{11}^2 + \beta_{22}X_{22}^2 + \beta_{33}X_{33}^2 + \beta_{12}X_1X_2 + \beta_{13}X_1X_3 + \beta_{23}X_2X_3 \quad \text{(Eq. 4.1)}$$

$$Y_{Active\ 5P12\text{-}Rantes} = \mu_\gamma + \gamma_1X_1 + \gamma_2X_2 + \gamma_3X_3 + \gamma_{11}X_{11}^2 + \gamma_{22}X_{22}^2 + \gamma_{33}X_{33}^2 + \gamma_{12}X_1X_2 + \gamma_{13}X_1X_3 + \gamma_{23}X_2X_3 \quad \text{(Eq. 4.2)}$$

$$Y_{\text{Specific Yield}} = \mu_\delta + \delta_1 X_1 + \delta_2 X_2 + \delta_3 X_3 + \delta_{11} X_{11}^2 + \delta_{22} X_{22}^2 + \delta_{33} X_{33}^2 + \delta_{12} X_1 X_2 + \delta_{13} X_1 X_3 + \delta_{23} X_2 X_3 \quad \text{(Eq. 4.3)}$$

The null hypothesis state that there is not quantifiable effect of $MeOH_{GR}$, T and pH in the overall responses 5P12-Ranres, Active 5P12-Rantes and Yield. If this hypothesis is true then:

$$H_{0\beta} : \beta_1 = \beta_{11} = 0,\ \beta_2 = \beta_{22} = 0,\ \beta_3 = \beta_{33} = 0,\ \beta_{12} = \beta_{13} = \beta_{23} = 0$$

$$H_{0\gamma} : \gamma_1 = \gamma_{11} = 0,\ \gamma_2 = \gamma_{22} = 0,\ \gamma_3 = \gamma_{33} = 0,\ \gamma_{12} = \gamma_{13} = \gamma_{23} = 0$$

$$H_{0\delta} : \delta_1 = \delta_{11} = 0,\ \delta_2 = \delta_{22} = 0,\ \delta_3 = \delta_{33} = 0,\ \delta_{12} = \delta_{13} = \delta_{23} = 0$$

The alternative hypothesis postulated that at least one of the coefficients is different to zero. Then:

$$H_{1\beta} : \text{At least one } \beta \neq 0$$

$$H_{1\gamma} : \text{At least one } \gamma \neq 0$$

$$H_{1\delta} : \text{At least one } \delta \neq 0$$

F-TEST

The F-test is a statistical test based on an F-distribution under the null hypothesis. The values obtained from the F-test will indicate the rejection or no rejection of the null hypothesis. F-calculated (F-calc) is determined from the ratio of the mean squares (MS) of factor, blocks, linear, factor squares and factor interactions and the error mean square (MSe). The F-critical (F-crit) is the value obtained from tables of critical values of F-distribution using the degrees of freedom of both numerator (df_n) and denominator (df_d).

The rejection or not rejection of the null variable is based in the comparison of the F-calc and F-crit. If the value of F-calc is greater than F-crit the null hypothesis is rejected. Otherwise it's not rejected.

P-VALUE

The P-value represents the probability of obtaining a value that is at least as the extreme as the calculated value if the null hypothesis is true. It has been assumed that 5% probability, α-value, is appropriate to evaluate the P-value. If the P-value is lower than the α value indicates the rejection of the null hypothesis.

METHODS

The RSM was analyzed using the software Minitab-16 (Minitab®). The analysis provides the corresponding ANOVA table for each response. Each response was evaluated under the null hypothesis. The ANOVA table provides the sum of squares (SS), the mean square (MS), the F-calc and the P-value. This analysis includes the evaluation for each independent factor, blocks, linear factors, quadratic factors, interaction and the error. The F-crit is obtained from tables of critical values F-distribution. The level of significance or α-value is 0.05. The data evaluated using ANOVA directs to the rejection of acceptance of the null hypothesis.

Table 4.1: ANOVA for the total amount of 5P12-Rantes with R-square = 89.01% and 3 factors

Source	DF	SS	MS	F-crit	F-calc	P-value	Reject $H_{0\beta}$
Blocks	2	423.49	156.58	4.46	1.45	0.290	No
MeOH	1	181.26	181.26	5.32	1.68	0.231	No
Temp	1	54.06	54.06	5.32	0.50	0.499	No
pH	1	125.06	125.06	5.32	1.16	0.313	No
$MeOH_{GR}$* $MeOH_{GR}$	1	60.30	301.98	5.32	2.80	0.133	No
Temp*Temp	1	1270.54	1757.38	5.32	16.31	0.004	Yes
pH*pH	1	4157.59	4157.59	5.32	38.58	0.000	Yes
$MeOH_{GR}$ *Temp	1	29.80	29.80	5.32	0.28	0.613	No
$MeOH_{GR}$ *pH	1	581.41	581.41	5.32	5.39	0.049	Yes
Temp*pH	1	102.39	102.39	5.32	0.95	0.358	No
Residual error	8	862.19	107.77				
Lack-of-Fit	5	860.40	172.08	9.01	287.73	0.000	Yes
Pure error	3	1.79	0.60				
Total	19	7848.08					

Table 4.2: ANOVA for the Active 5P12-Rantes with R-square = 86.26% and three factors

Source	DF	SS	MS	F-crit	F-calc	P-value	Reject $H_{0\gamma}$
Blocks	2	106.26	39.893	4.46	1.12	0.373	No
$MeOH_{GR}$	1	1.81	1.811	5.32	0.05	0.827	No
Temp	1	75.12	75.121	5.32	2.11	0.185	No
pH	1	183.39	183.389	5.32	5.14	0.053	No
$MeOH_{GR}$*$MeOH_{GR}$	1	42.49	120.273	5.32	3.37	0.104	No
Temp*Temp	1	276.46	382.052	5.32	10.72	0.011	Yes
pH*pH	1	899.41	899.408	5.32	25.23	0.001	Yes
$MeOH_{GR}$ *Temp	1	20.00	20.003	5.32	0.56	0.475	No
$MeOH_{GR}$ *pH	1	147.32	147.319	5.32	4.13	0.077	No
Temp*pH	1	37.45	37.455	5.32	1.05	0.335	No
Residual error	8	285.18	35.647				
Lack-of-Fit	5	270.89	54.178	9.01	11.37	0.036	Yes
Pure error	3	14.29	4.763				
Total	19	2074.90					

Table 4.3: ANOVA for the Specific Yield (Total 5P12-Rantes (mg)/dry cells (g)) with R-square = 88.07% and three factors

Source	DF	SS	MS	F-crit	F-calc	P-value	Reject $H_{0\delta}$
Blocks	2	0.00166	0.00083	4.46	0.93	0.434	No
$MeOH_{GR}$	1	0.00051	0.00051	5.32	0.57	0.471	No
Temp	1	0.01404	0.01404	5.32	15.7	0.004	Yes
pH	1	0.00758	0.00758	5.32	8.48	0.020	Yes
$MeOH_{GR}$*$MeOH_{GR}$	1	0.00233	0.00233	5.32	2.61	0.145	No
Temp*Temp	1	0.01378	0.01378	5.32	15.41	0.004	Yes
pH*pH	1	0.03241	0.03241	5.32	36.25	0.000	Yes
$MeOH_{GR}$*Temp	1	0.00054	0.00054	5.32	0.6	0.460	No
$MeOH_{GR}$*pH	1	0.00295	0.00295	5.32	3.3	0.107	No
Temp*pH	1	0.00106	0.00106	5.32	1.19	0.308	No
Residual	8	0.00715	0.00089				
Lack-of-Fit	5	0.00682	0.00136	9.01	12.15	0.033	Yes
Pure	3	0.00034	0.00011				
Total	19						

RESULTS AND DISCUSSION

The tables 4.1, 4.2 and 4.3 show “lack of fit” of the model. The P-value is lower than the 0.01 level for the total amount of 5P2-Rantes. In addition, the P-values for both the active 5P12-Rantes and specific yield are at the 0.05 level of significance. The elevated level of significance indicates that the proposed model doesn’t accurately predict the responses. However, The result obtained from the significance analysis does not mean that the experiments are not run properly or that the data obtained is incorrect. It is more accurate to conclude that the responses are very complex that cannot be fit using a second order design.

The evaluation of the each proposed model directs to conclude that temperature and pH have a great significance in the responses. Conversely, The Methanol growth rate ($MeOH_{GR}$) does not have significant effect in the responses. In consequence, this factor is excluded out of the model to decrease the significance in the lack of fit.

A new model with 2 factors at 5 levels each is proposed. Temperature and pH are used to evaluate the responses. It is noticeable form tables 4.5 and 4.6 that the lack of fit has decreased for the active 5P12-Rantes and for the specific yield responses. However, table 4.4 shows that the lack of fit for the 5P12-Rantes remains significant.

Table 4.4: ANOVA for 5P12-Rantes with R-square of 81.24% and two factors

Source	DF	SS	MS	F-crit	F-calc	P-value	Reject $H_{0\beta}$
Blocks	1	16.12	16.12	6.61	0.07	0.799	No
Temp	1	1841.60	1841.60	6.61	8.25	0.035	Yes
pH	1	762.22	762.22	6.61	3.42	0.124	No
Temp*Temp	1	1769.20	1769.20	6.61	7.93	0.037	Yes
pH*pH	1	3779.43	3779.43	6.61	16.94	0.009	Yes
Temp*pH	1	71.49	71.49	6.61	0.32	0.596	No
Residual error	5	1115.64	223.13				
Lack-of-Fit	3	1114.16	371.39	5.41	501.16	0.002	Yes
Pure error	2	1.48	0.74	4.46			
Total	11	5947.83					

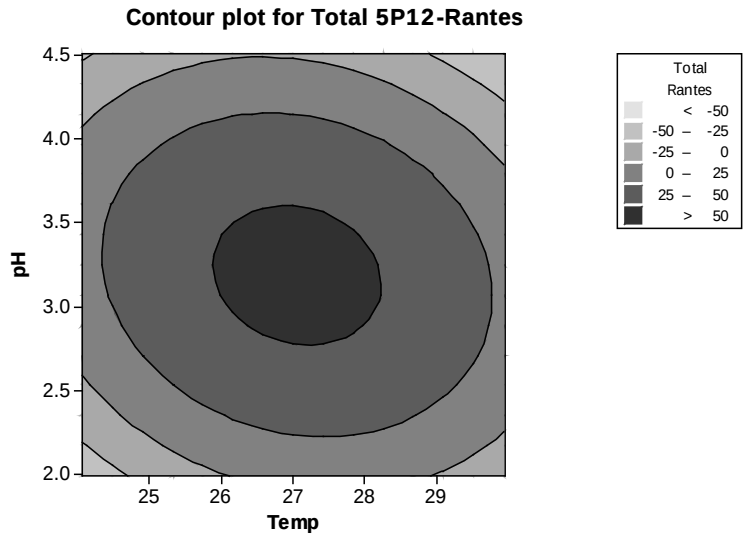

Figure 4.1.: Contour plot for the total 5P12-Rantes

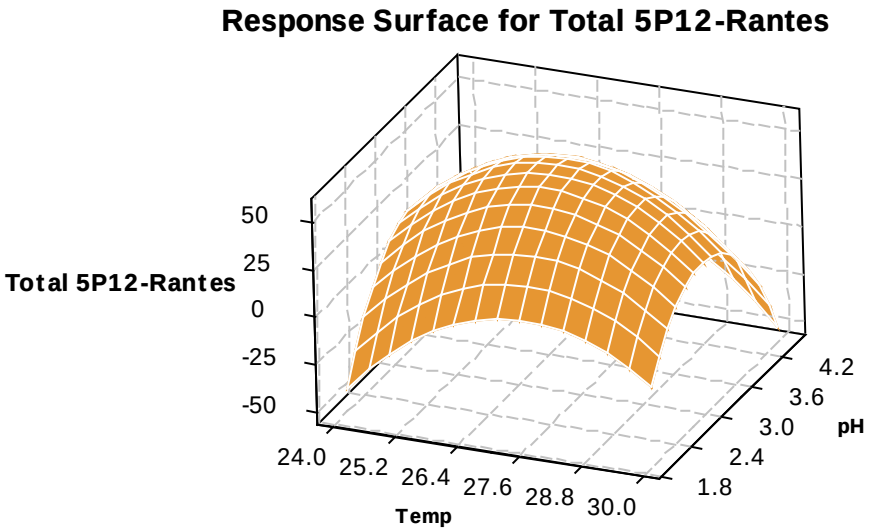

Figure 4.2: Surface response for the total 5P12-Rantes

Table 4.5: ANOVA for Active 5P12-Rantes with R-square of 85.88% and two factors

Source	DF	SS	MS	F-crit	F-calc	P-value	Reject $H_{0\beta}$
Blocks	1	0.25	0.250	6.61	0.01	0.939	No
Temp	1	445.47	445.466	6.61	11.62	0.019	Yes
pH	1	121.40	121.400	6.61	3.17	0.135	No
Temp*Temp	1	449.38	449.381	6.61	11.72	0.019	Yes
pH*pH	1	911.28	911.283	6.61	23.77	0.005	Yes
Temp*pH	1	2.34	2.341	6.61	0.06	0.815	No
Residual error	5	191.71	38.343				
Lack-of-Fit	3	178.85	59.617	5.41	9.27	0.099	No
Pure error	2	12.86	6.431	4.46			
Total	11	1357.68					

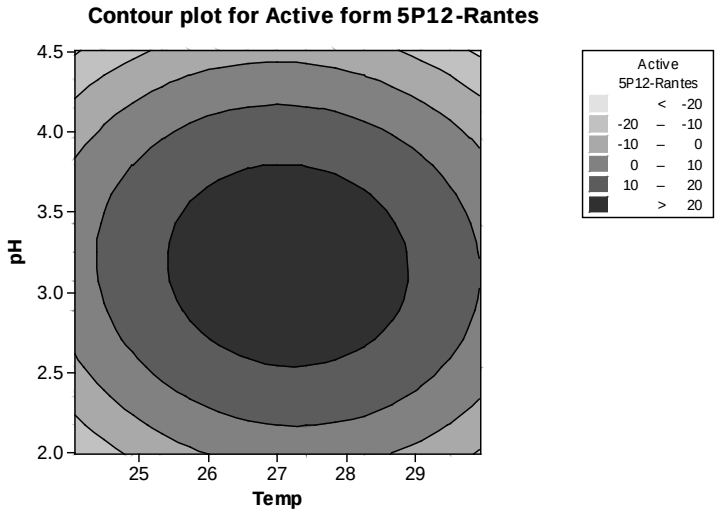

Figure 4.3: Contour plot for the active 5P12-Rantes

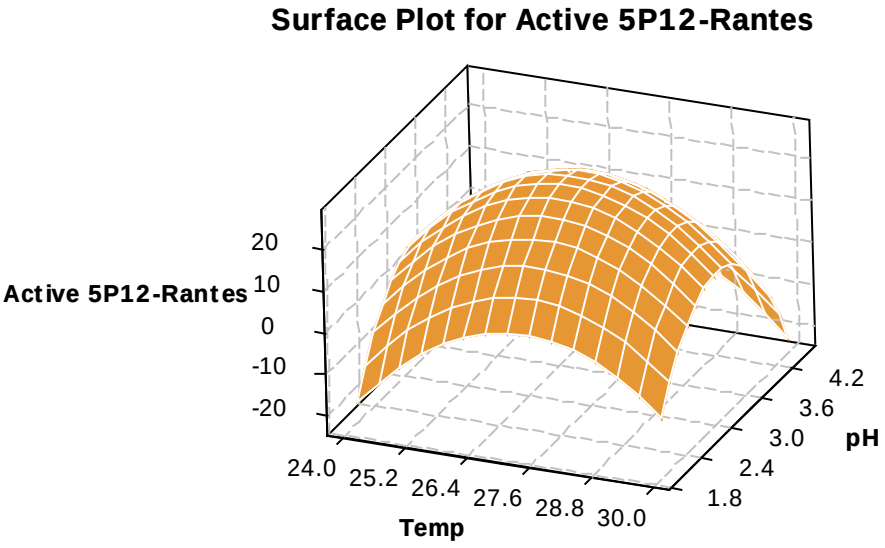

Figure 4.4 : response surface for the active 5P12-Rantes

Table 4.6: ANOVA for Active 5P12-Rantes with R-square of 81.35% and two factors

Source	DF	SS	MS	F-crit	F-calc	P-value	Reject $H_{0\beta}$
Blocks	1	0.000053	0.000053	6.61	0.03	0.87	No
Temp	1	0.014738	0.014738	6.61	8.25	0.035	Yes
pH	1	0.005794	0.005794	6.61	3.24	0.132	No
Temp*Temp	1	0.014135	0.014135	6.61	7.91	0.037	Yes
pH*pH	1	0.029859	0.029859	6.61	16.72	0.009	Yes
Temp*pH	1	0.000520	0.000520	6.61	0.29	0.613	No
Residual error	5	0.008930	0.001786				
Lack-of-Fit	3	0.008638	0.002879	5.41	19.68	0.05	No
Pure error	2	0.000293	0.000146	4.46			
Total	11	0.047876					

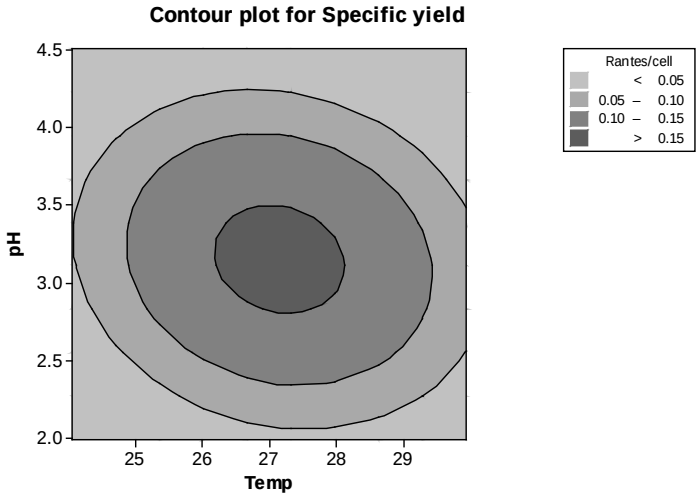

Figure 4.5: Contour plot for Specific yield

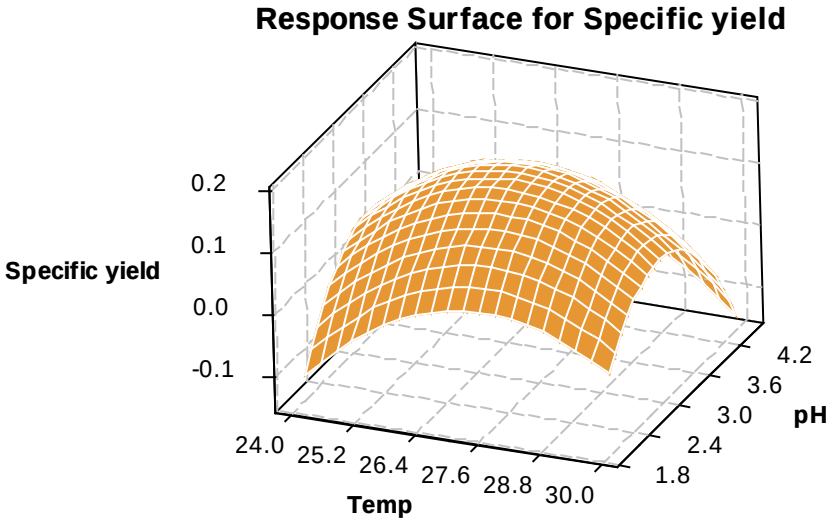

Figure 4.6: Surface response for specific yield

REFERENCES

Ghosalkar, A., Sahai, V., Srivastava, A. (2008) Optimization of chemically defined médium for recombinant Pichia pastoris for biomass producción, Bioresource technology, 99, 7906 – 7910.

Hao, X-C., Yu, X-B., Yan, Z-L., (2006) Optimization of the medium for the production of cellulose by the mutant trichoderma reesei WX-112 Using Response Surface Methodology. Food Technology and Biotechnology, 44, 89-94.

Inan, M., Chiruvolu, V., Eskridge, K., Vlasuk, G., Dickerson, K., Brown, S., Meagher, M., (1999) Optimization of temperature-glycerol-pH conditions for a feed-batch fermentation process for recombinant hookworm (Ancylostoma caninum) anticoagulant peptide (AcAP-5) production by Pichia pastoris, Enzyme and Microbial Technology, 24, 438-435.

Liu, M., Potvin, G., Huang, Z., Zhang, Z., (2011) Medium Optimization for the production of Phytase by Recombinant Pichia pastoris growth on glycerol, International Journal od Chemical Reactor Engineering, 9, 1-16

Myers, R., Response Surface Methodology, Edwards Brothers, Ann Arbor, MI, 1976

Parampalli, A., Eskridge, K., Smith, L., Meagher, M., Mowry, M., Subramanian, A., (2007) Development of serum-free media in CHO-DG44 cells using a central composite statistical design. Cytothecnology,54,57-68

Walpole, R., Myers, R., Myers, S., Ye K., (2007) Probability and Statistics for engineers and scientist, Prentice Hall, Upper Saddle River, NJ, 8th edition

Zhang, W., Liu, C-P., Inan, M., Meagher, M., (2004) Optimization of cell density and dilution rate in Pichia pastoris continuous fermentation for production of recombinant proteins, Journal Industrial Microbiology and Biotechnology, 31, 330-334.

CHAPTER V

RESULTS AND DISCUSSION

The clonal linage used in this research express the un-cyclized form of 5P12-Rantes. The formation of the active of 5P12-Rantes for is produced in the Golgi compartment when the translated protein is detached from the secretory signal (α-mating factor) by the KEX2 protease. The formation of the pyro-glutamic acid (pyro-Q) at the N-terminal of 5P12-Rantes during fermentation is not an enzymatic reaction. The pyro-Q is catalyzed by temperature during fermentation (table 4.5). The cyclization reaction is not reversible. 5P12-Rantes protein is stable at the active form. The formation of the two disulfide bonds is enhanced by the *P. pastoris* protein disulfide isomerase.

The results obtained from the ANOVA for each response using a second order model with 3 factors at 5 levels indicate “lack of fit” of the proposed models. As indicated previously, this lack of fit of the models indicates the complexity of the system in which the 5P12-Rantes expression is evaluated. The outcomes obtained from this analysis enable the evaluation of the effects of Methanol growth rate ($MeOH_{GR}$), Temperature and pH. This evaluation demonstrates that $MeOH_{GR}$ is not a significant factor in the final responses. Conversely, temperature and pH have an important effect over the final responses.

In order to decrease the lack of fit of the proposed models; a strategy is applied by decreasing the number of factors involved in the responses. Since $MeOH_{GR}$ has no effect in the final response, this factor can be excluded out of the model. Thus, a new design is constructed using temperature and pH.

The final outcome using the second order design with 2 factors at 5 levels each confirms the decrease in the lack of fit for both the Active 5P12-Rantes and specific yield responses. However, the lack of fit for the total 5P12-Rantes is recurrent and reflexes the complexity of the response against the proposed model.

It is noticeable that the R-square value for the 3 responses drops from 89.01% to 81.24% for the total 5P12-Rantes, from 86.26% to 85.88% for the Active 5P12-Rantes and from 88.07% to 81.35% for the specific yield. This is due to the amount of factors used to predict the behavior of the response.

The models proposed to explain and predict the expression of active 5P12-Rantes and specific yield are:

$$Y_{\text{Active 5P12-Rantes}} = - 1755.88 + 117.229\ X_1 + 120.224\ X_2 - 2.124\ X_{11}^2 - 16.468\ X_{22}^2 - 0.584\ X_1X_2$$

$$Y_{\text{Specific Yield}} = - 10.3011 + 0.6743\ X_1 + 0.8306\ X_2 - 0.0119\ X_{11}^2 - 0.0943\ X_{22}^2 - 0.0087\ X_1X_2$$

The optimal values for temperature and pH at which the maximum expression is reached determined using Minitab 16:

Response	Temperature °C	pH	Maximum Outcome
Active 5P12-Rantes	27.14	3.16	26.52 g/L
Specific yield	27.14	3.16	0.161 mg 5P12-Rantes/g cell

Nevertheless the effect of methanol is disregarded from the proposed model, it is important to consider that a growth rate at or above 0.8 h^{-1} will exceed the maximum capacity of the cell to metabolize methanol and methanol will have detrimental effect on the cell growth as indicated by Zhang (2000).

Reference

Zhang, W., Bevins, M., Plantz, B., Smith, L., Meagher, M., (2000) Modeling Pichia pastoris on methanol and optimizing the production of a recombinant protein, the heavy-chain fragment C of botulinum neurotoxin, serotype A, Biotechnology and Bioengineering, 70, 1-8.

FUTURE STUDIES

1. Evaluate the contribution of dissolve oxygen in the responses.
2. Evaluate the action of the enzyme glutaminyl cyclase in the formation of pyro-glutamic acid for the active for of 5P12-Rantes during fermentation.